CHAPTER 5

Novel imidazolium-based ionic discotic liquid crystalline dimers and polymers

5.1 Introduction

In the previous chapter, we described conventional low molar mass ionic liquid crystals particularly imidazolium- and pyridinium-based ionic liquids. Recently, however, interest has grown concerning non-conventional liquid crystals [1] and the influence of the ionic character upon mesomorphic properties [2]. The physical properties of non-conventional liquid crystals (liquid crystalline dimers, oligomers and polymers) are significantly different from those of conventional low molar mass mesogens because of restricted molecular motion. This chapter mainly concerned with the synthesis and characterization of some ionic liquid crystalline dimers and polymers.

Compare to the large number of calamitic and discotic ionic molecules as mentioned in chapter 4, only a few ionic liquid crystalline dimers and polymers are known. For example, Veber and co-workers reported dimeric 2, 4, 6-triarylpyrilium tetrafluoroborate **(1a, 1b)** and symmetrically substituted ionic liquid crystalline dithiolium salts **(2)** [3, 4]. Whereas, the pyrilium salts show a hexagonal columnar mesophase, dithiolium salts exhibit a smectic mesophase. Ionic metallomesogens composed of two mesogenic units, have been extensively studied. For example Bruce and co-workers [5] showed that the silver(I) complexes of substituted alkoxystilbazoles **(3)** form two coordinate linear complexes with a remarkably rich mesomorphism.

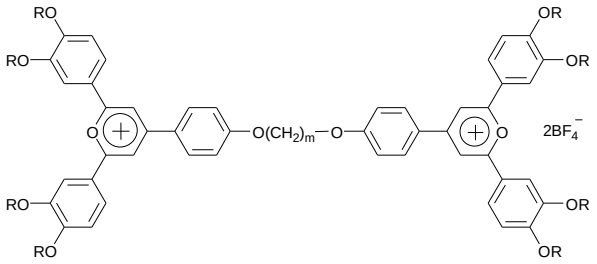

1a

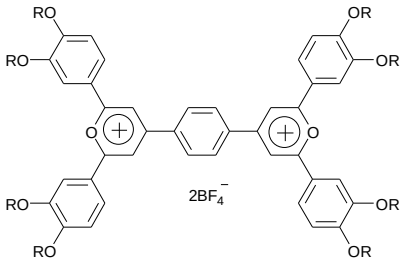

1b

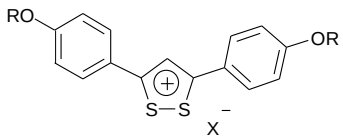

2

These mesogens show interesting mesomorphic behaviour depending upon fluorine substitution on the aromatic core [6]. On substitution of fluorine at the 3 position **(4)** of the structure **3** stabilised the smectic A phase but destabilized the nematic phase. A different behaviour was observed for the complexes with a fluorine substituent at the 2 position **(5)**. Here both the nematic phase and cubic phase were promoted at the expense of the SmA phase. Tetracatenar silver(I) dodecyl sulfate complexes of 3, 4-dialkoxystilbazoles **(6)** show a hexagonal columnar phase and cubic phase [7]. Serrano and co-workers investigated a series of silver (I) complexes of 4-substituted pyridines **(7)**. Similar dimers but having –COO linking group instead of –CN group **(8)** was studied by Bruce and co-workers [8]. Most of the complexes showed a smectic A phase. On the other hand, silver(I) complexes of polycatenar bent core pyridines **(9)** display hexagonal and rectangular columnar phases [9].

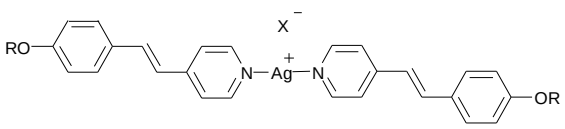

3

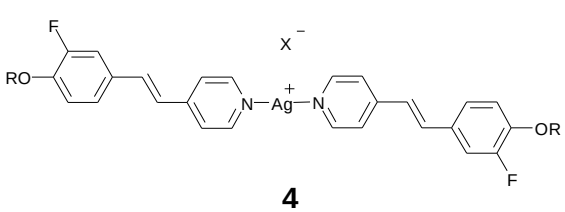

4

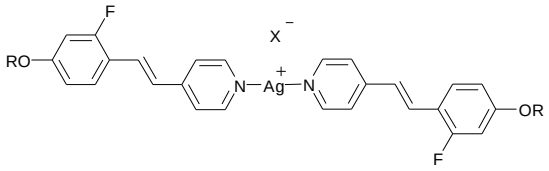

5

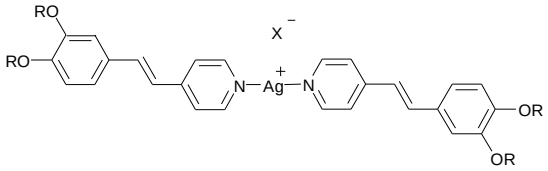

6

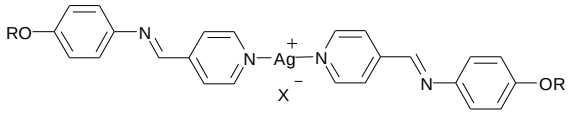

7

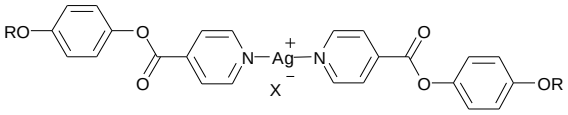

8

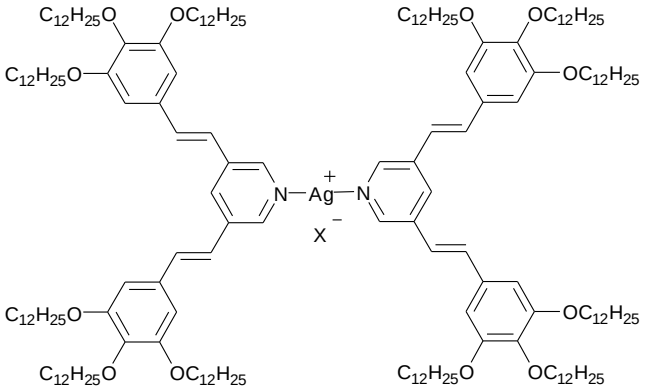

9

For many years, ionic liquid crystalline polymers with the mesogen in the main chain or in the side group have been investigated intensively, for their scientific and technological potentials [10]. For example, Hara and co-workers [11] developed main chain polymer liquid crystals by introducing ionic groups into the polymer chain to obtain better tensile and compressive properties. They have chosen a wholly aromatic polyester based on random

copolymerization of 4-hydroxybenzoic acid, 6-hydroxy-2-napthoic acid, a 5-sulfoisophthalate salt and hydroquinone **(10)**.

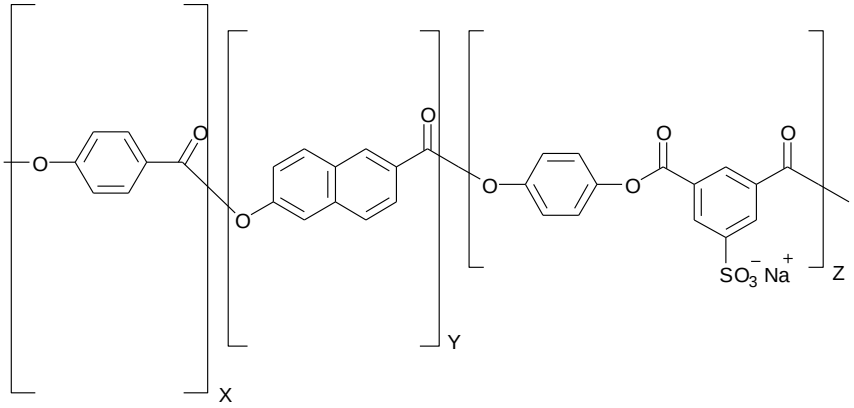

10

Paleos and co-workers investigated the mesomorphic properties of oligomeric viologens **(11)** [12]. Main chain liquid crystalline viologen polymers (**12**) have been intensively studied by Bhowmik et al [13]. These compounds exhibit both thermotropic and lyotropic mesomorphism. The thermotropic phases were identified as smectic phases. These polymers have some interesting properties such as electric conductivity, electrochromism, photochromism and thermochromism. Another type of viologen polymers **(13)** was prepared by the reaction between 4,4'-bipyridine with the ditosylate of trans-1,4-cyclohexanedimethanol [14]. Also viologen polymers with ortho-, meta- and para-xylyl units in the backbone, and with bromide, tosylate or teiflimide counter ions **(14a, 14b, 14c)** are known [15]. Subsequently, several others main chain ionic polymers have been prepared and studied extensively [16]. Bazuin and co-workers investigated tail-end amphiphiles of the type poly(ω-pyridinium alkyl methacrylates) **(15)** with various 4-substituted pyridinium bromide groups [17]. Haramoto and co-workers described high molecular weight ionic liquid crystalline polymers with a 4-(1,3-dioxan-2-yl) pyridinium group **(16)** [18].

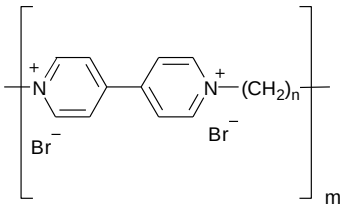

11

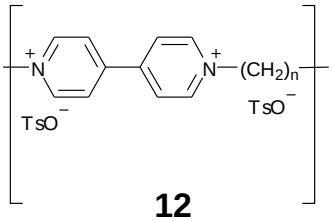

12

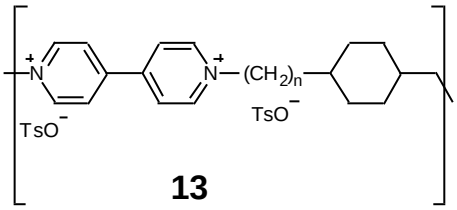

13

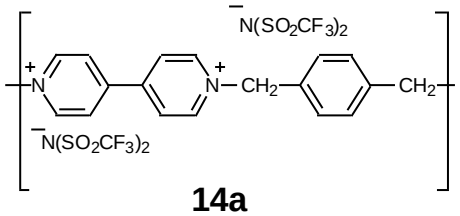

14a

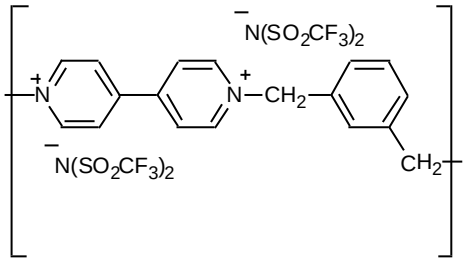

14b

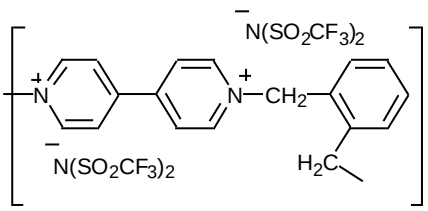

14c

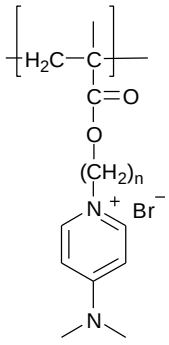

15

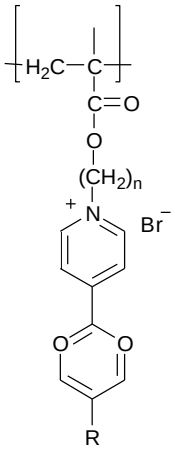

16

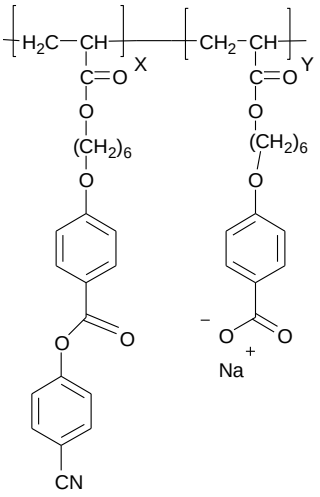

17a

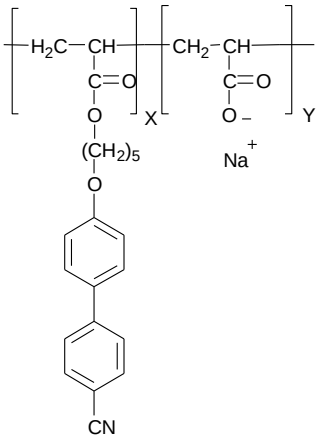

17b

Ionic side chain polymers with sodium counter ion **(17a, 17b)** are also reported [19]. Side chain liquid crystalline polymers bearing à 15-crown-5 **(18)** unit exhibit interestingly both SmA and N phase [20].

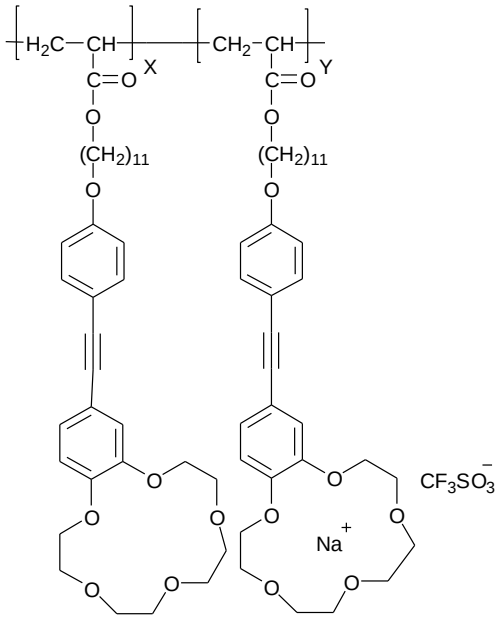

18

Barmatov and co-workers investigated liquid crystalline ionomers containing alkali metal ions, alkaline-earth metal ions, transition metal ions and rare-earth ions to establish the effect of the nature of the metal ion on the mesophase behaviour [21]. Poly(4-vinylpyridinium) salts with cyanobiphenyl, chiral biphenyl, (4-methoxy-4'-biphenyloxy) alkyl halide as mesogenic units are also reported to show interesting phases [22]. Similarly ionic polysiloxane, poly(ethylene imine) polymers bearing calamitic mesogenic units are also known in literature [23].

Polymer consisting of a triphenylene unit has been well explored. The Ringsdorf group [24] reported side chain discotic polysiloxane **(19a**, **19b)** with pentasubstituted triphenylene rings attached to the backbone via flexible spacers with ethers or esters as a linking group.

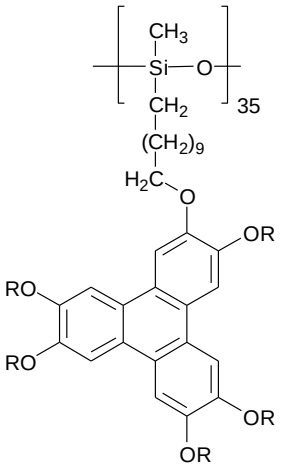

19a

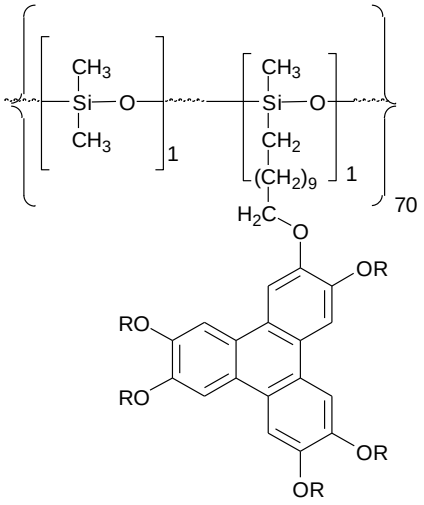

19b

Suitably substituted triphenylene polyacrylates **(20)** and polymethycrylates **(21)** have been extensively studied [25]. Recently Imrie and co-workers prepared triphenylene-based side chain polymer **22** by melt polycondensation of the triphenylene substitute isophthalate with polyethylene glycol (PEG 300) [26].

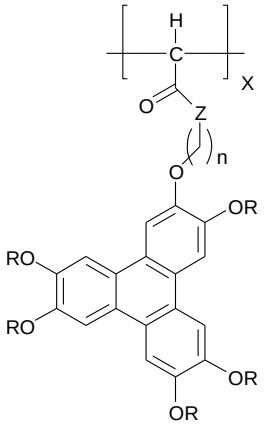

20

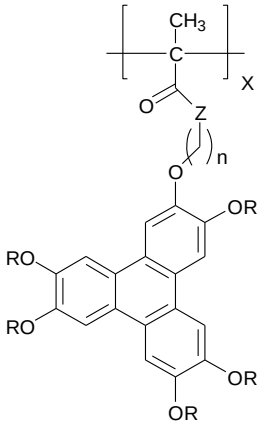

21

The polycondensation of malonic acid diethyl ester with the 2, 3-difunctionalized triphenylene derivative afforded polymer **23** [27]. In contrast to the majority of triphenylene-based polymers, it shows a discotic nematic phase between the glass transition at -10ºC and isotropic transition at 31ºC. The chemistry of triphenylene-based discotic dimers, oligomers and polymers has recently been covered in a review article [28].

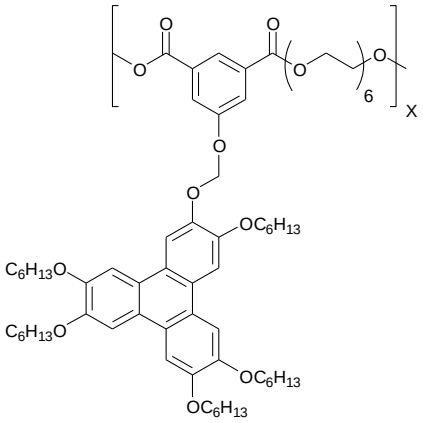

22

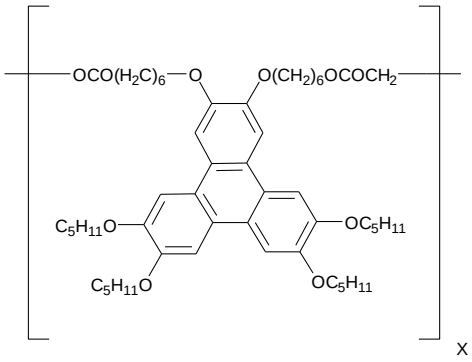

23

5.2 Objective

One of the recent advances in the molecular electronics is to search for the elusive ion-conductive materials, to be used at a molecular level, for which the ion conductivity should be

anisotropic, which means that the ion conductivity depends on the direction in which it is measured. Ionic liquid crystals are the most promising candidates to design anisotropic ion-conductive materials because they have an anisotropic structural organization and also they contain ions as charge carriers. Moreover, the long alkyl chains of mesogenic molecules can act as an insulating sheet for the ion conductive channel. Liquid crystals with a columnar mesophase can be used to prepare a material for one dimensional ion-conduction. Triphenylene derivatives are the archetypal discotic liquid crystals. Highly ordered columnar mesophase formed by triphenylene-based ionic liquid crystals may give a high anisotropy of the system which may be responsible for tremendous ion conduction. Obviously, they will be the good candidates in molecular electronics. To make these types of materials on the basis of ionic liquid crystals that keep their anisotropic ion conductivity for a long time it is necessary to stabilize the ordered molecular arrangement of the liquid crystalline monodomain. Ionic dimeric and polymeric liquid crystals are the representatives of this type of systems**.**

To the best of our knowledge ionic liquid crystalline dimers based on imidazolium moiety containing two mesogenic groups and ionic discotic liquid crystalline polymers based on triphenylene has not yet been explored in literature. Hybridisation of two different types of mesogens with imidazolium moiety may lead to novel materials with interesting properties. With this in mind, we have initiated this research programme to incorporate imidazolium-based ionic liquids in the supramolecular order of calamitic and discotic liquid crystals by attaching two calamitic, two discotic and hybrid of both the moieties, to imidazole. Microwave dielectric heating was used to prepare these dimers. Similarly, we have prepared ionic discotic polymer for the first time which is very useful for unidirectional transport of ion and energy at nanoscale.

5.3 Synthesis

The synthesis of imidazolium-based calamitic-calamitic ionic dimers is outlined in scheme 1. Commercially available 4'-hydroxy-4-biphenylcarbonitrile **24** was alkylated under classical conditions with an excess of the appropriate α,ω-dibromoalkane to obtain the ω-brominated product **25** [29]. Imidazole-substituted alkoxycyanobiphenyl **26** was obtained by reacting **25** with imidazole in presence of NaH. Liquid crystalline imidazolium salt **27** was obtained by quaternization of **26** with methyl iodide. Ionic liquid crystalline calamitic-calamitic dimers **28** were obtained by attaching one more molecule of ω-brominated cyanobiphenyl to the imidazole substituted moiety **26**.

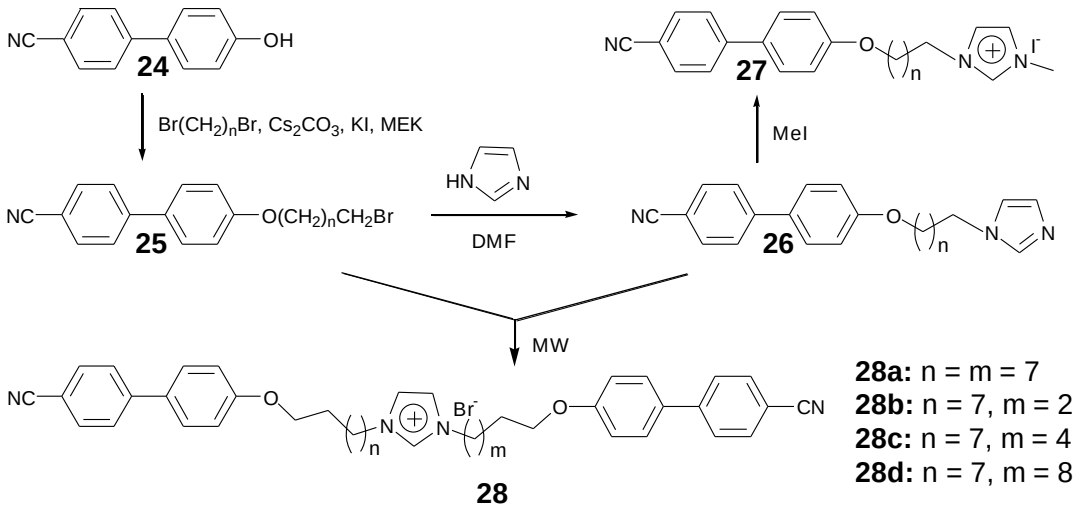

Scheme 1. Synthesis of imidazolium-based calamitic-calamitic dimers

Thus quaternization of **26** with ω-bromoterminated cyanobiphenyl under microwave irradiations furnished the dimers **28** in about 1 minute. It should be noted that attempted quaternization under classical reaction conditions like reflux in toluene for 48 hours did not produce any desired product. Similarly, calamitic-discotic imidazolium salt **30** was obtained (scheme 2) by attaching one molecule of ω-bromoterminated triphenylene **29** to the imidazole-substituted moiety **26**. The

ω-brominated triphenylene **29** was obtained from monohydroxy triphenylene as already reported in literature [30]. Discotic-discotic ionic salt was obtained by quaternization of **31** with ω-bromoterminated triphenylene **29** under microwave dielectric heating within one minute (scheme 2). The detailed synthetic procedure has been given in experimental section.

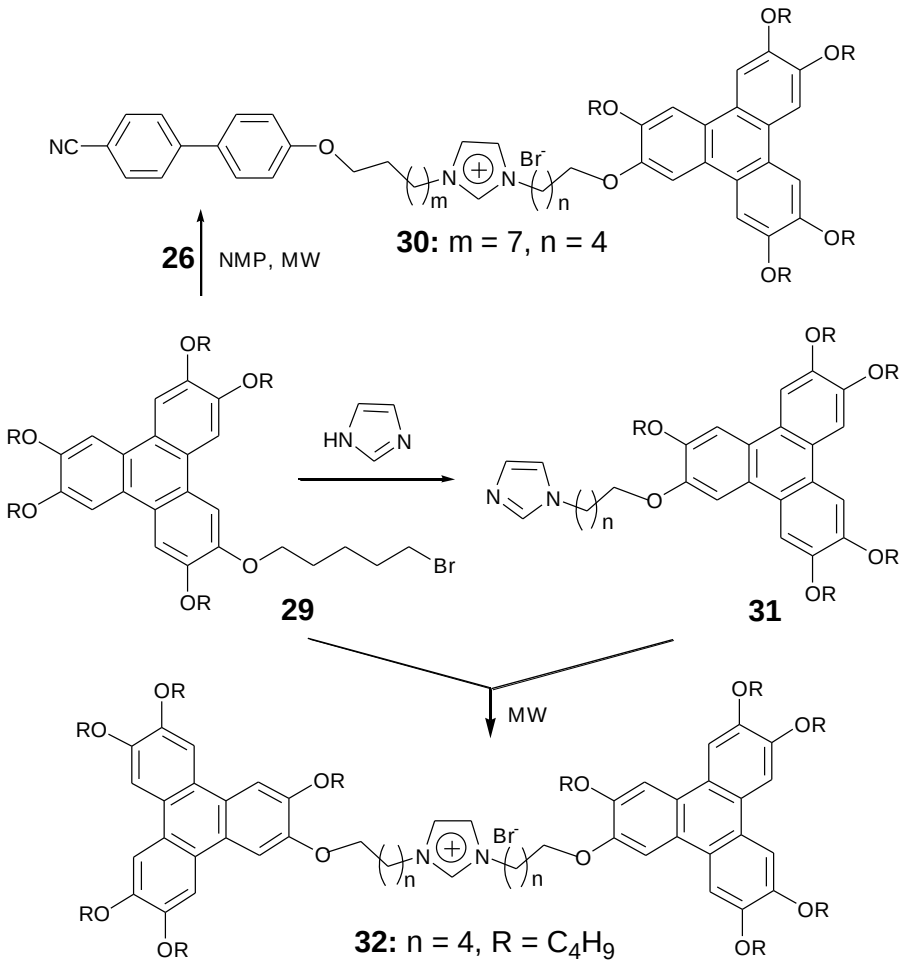

Scheme 2

Scheme 2. Synthesis of imidazolium-based calamitic-discotic and discotic-discotic dimers.

5.4 Characterization

All the compounds were purified by repeated column chromatography followed by crystallization and characterized from their ^{1}H NMR, IR, UV spectra and elemental analysis. All

the members of the series give similar spectra. Spectral data and elemental analysis of all the compounds were in good agreement with their structures, indicating the high purity of all the materials. Characterization of ω-bromoterminated cyanobiphenyl has already been described in chapter 2.

Figure 1 represents the ^{1}H NMR of the compound **26** (n = 8). There are seven types of aromatic protons assigned as H_a to H_g on the structure below.

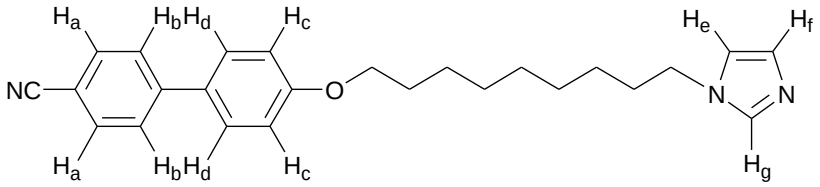

26 (n = 8)

As can be seen from the structure above, protons which are ortho to –CN group (H_a) are in the same environment and have the same δ values. These protons couple with the neighboring H_b protons and appear as doublet (d) and vice-versa. As they are (H_a, H_b) attached to aromatic ring having strongly electron withdrawing –CN group they have δ values higher compare to other hydrogens. Having ortho to –CN group H_a protons have highest δ values (δ = 7.7) in comparison to H_b protons (δ = 7.6) and obviously, with respect to all other hydrogens. Similarly H_c and H_d protons appear as doublet with δ values 7.5 and 6.9 respectively. H_g protons appear as singlet at a δ value of 7.5 ppm. H_e and H_f protons resonate at δ 7.0 and 6.9 ppm, respectively and appear as a singlet in the NMR spectrum. The $–NCH_2$ and $–OCH_2$ protons resonate with δ values of 3.9 and 4.0 ppm respectively and appear as a triplet in the spectrum. Other aliphatic protons of the chains can be clearly seen in the spectrum in between δ 1.0 ppm to 2.0 ppm. This confirms the structure and high purity of the compound.

Figure 2 represents the ^{1}H NMR of the compound **27** (n = 8). Proton H_g is flanked between two strong electronegative nitrogen atoms and therefore, appear at the highest δ value compare to other hydrogens as evident clearly in the NMR spectrum (δ = 10.1 ppm).

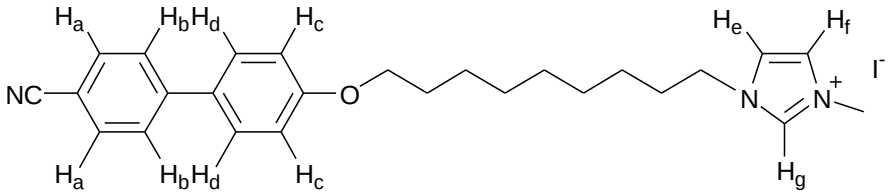

27

As explained earlier proton H_a and H_b appear as doublet (d) with δ values 7.7 and 7.6 respectively. Similarly, H_c and H_d protons appear as doublet with δ values 7.5 and 6.9 respectively. H_e and H_f protons appear as a singlet at δ 7.23 and 7.26 (merged with $CDCl_3$) ppm. The $–NCH_2$ and $–OCH_2$ protons resonate with δ values of 4.32 and 4.00 ppm respectively and appear as a triplet in the spectrum. The $N^+C\underline{H}_3$ proton appear as singlet with a δ value of 4.1 ppm. Other aliphatic protons of the chains can be clearly seen in the spectrum in between δ 1.2 ppm to 2.0 ppm. This confirms the structure and high purity of the compound.

Figure 3 represents the ^{1}H NMR of **28a**. There are six different types of aromatic protons assigned as H_a to H_f on the structure given below.

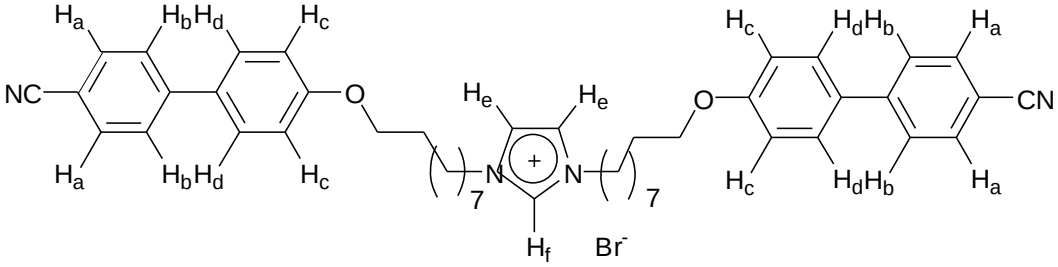

28a

As expected from the structure above, proton H_f is flanked between two strong electronegative nitrogen atoms and therefore, appear at the highest δ value compare to other hydrogen's as evident clearly in the NMR spectrum (δ = 10.5 ppm). Having ortho to –CN group H_a protons have δ values (δ = 7.7) higher in comparison to H_b protons (δ = 7.6). Similarly H_c and H_d protons appear as doublet with δ values 7.5 and 6.9 ppm, respectively. Protons H_e appears as a singlet with a δ value of 7.23 ppm near $CDCl_3$. The $–NCH_2$ and $–OCH_2$ protons resonate at δ 4.32 and 3.96 ppm, respectively and appear as a triplet in the spectrum. Other aliphatic protons of the chains can be clearly seen in the spectrum in between 1.0-2.0 ppm. This confirms the structure and high purity of the compound.

Figure 4 represents the ^1H NMR of compound **28b**. Due to unsymmetrical nature of this compound around the central imidazolium moiety, four triplets appear from the $–NCH_2$ and $–OCH_2$ part. Other aromatic and aliphatic hydrogens resonate almost at the same position as described earlier.

All the compounds exhibited satisfactory elemental analysis (within +/- 0.4 % of the theoretical values). The elemental analysis data are given in the experimental section.

Figure 5 shows the IR spectrum of the compound **28a**, which shows expected aromatic and aliphatic stretching. A strong peak is observed for –CN group at 2200 cm^{-1}.

The UV spectra of all the samples were measured in CH_2Cl_2 and similar spectrum is obtained for all the compounds (**28a-d**). Figure 6 represents the UV-Vis spectrum of the compound **28a**. It shows the major absorption at 307.6 nm.

Figure 7 represents the ^1H NMR of compound **30**. Due to asymmetry nature of the two mesogenic groups attached to the central imidazolium core, the H_e and H_f protons appear at δ

7.09 and 7.21 ppm. The H_g proton appears at the highest δ value (10.8 ppm). The triphenylene protons (H) appear as a multiplet (m) with a δ value of 7.82 ppm.

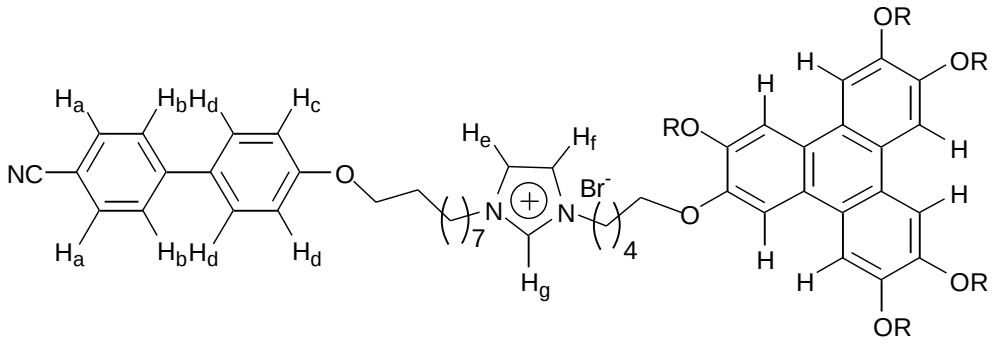

30

All the aromatic hydrogens in cyanobiphenyl ring (H_a, H_b, H_c, H_d) will appear as a doublets with δ values 7.68, 7.62, 7.51 and 6.96 ppm respectively. The two $–NCH_2$ protons, one attached to triphenylene unit and other with cyanobiphenyl moiety come as a triplet with δ values 4.45 and 4.29 ppm respectively. All $–OCH_2$ protons in triphenylene unit appear as a multiplate with a δ value of 4.25 ppm. The $–OCH_2$ protons attached to the cyanobiphenyl moiety resonate at a lower δ value of 3.95 ppm and clearly show triplets in the NMR spectrum. All other aliphatic hydrogens can be clearly seen in the spectrum in between δ 0.9-2.1 ppm.

Figure 8 shows the IR spectrum of compound **30**, which shows expected aromatic and aliphatic stretchings. A strong peak is observed for –CN group at 2200 cm^{-1}.

The UV spectrum of the compound **30** was measured in CH_2Cl_2. It shows absorption peaks at 266, 278, 305 nm. The UV-Vis spectrum of the compound **30** is reproduced in figure 9.

Characterization of compound **31** is described in chapter 4.

Figure 10 represents the ^1H NMR of compound **32**. There are only three types of aromatic protons which give rise to three signals at different δ values.

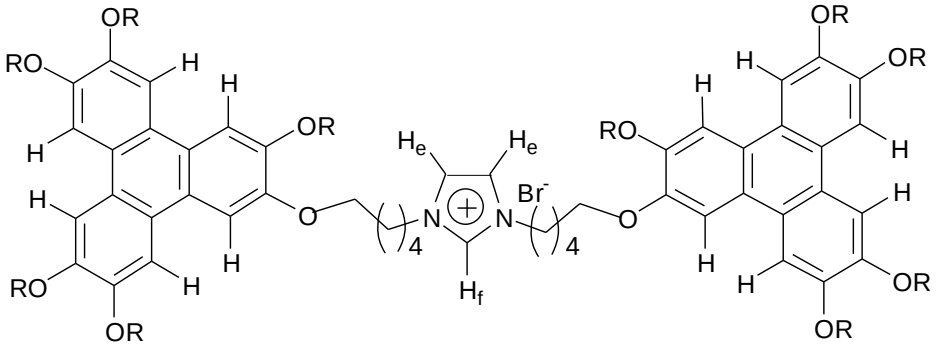

32

As shown in the structure above, the protons H_e and H_f in central imidazolium moiety appear as a singlet with δ values 7.19 and 10.77 ppm respectively similar to other calamitic-calamitic and calamitic-discotic salts, as discussed above. The triphenylene protons similarly appear as multiplates in the spectrum. All other aliphatic hydrogens can be clearly seen in the NMR spectrum. This supports the high purity of the material prepared by microwave-assisted synthesis.

IR and UV spectrum of compound **32** is reproduced in figure 11 and 12. The IR spectrum gives expected aromatic and aliphatic stretchings while the UV absorption occurs at 344.4, 305.2, 278.2, 269.6, 259 nm.

5.5 Thermal behavior

The phase transition temperatures of all the new compound together with the transition enthalpy values determined by DSC are given in table 1. The transition temperatures and associated enthalpy values were determined using a differential scanning calorimeter (DSC) which was operated at a scanning rate 5 ºC min^{-1} both on heating and cooling. The textural observation of the mesophase was carried out using polarizing light microscopy (POM) provided with a heating stage and a central processor. The dimer series based on calamitic-calamitic moiety displayed

SmC & SmA phases. Interestingly, calamitic-discotic hybrid **30** was found to be non-liquid crystalline. On the other hand dimer based on discotic-discotic moiety **32** showed a typical spine texture which compared well with the texture of columnar phases shown by several other discotic liquid crystals.

Table 1: Phase transition temperatures (peak, ºC) and associated enthalpy changes (KJ mol^{-1}, in parentheses) of imidazolium-based ionic and non-ionic mesogens. Cr: Crystalline phase; SmC: Smectic C phase; N: Nematic phase; SmA: Smectic A phase; I: Isotropic phase.

Compound	Heating scan	Cooling Scan
27	Cr 73 (4.3) Cr 83 (1.4) Cr 92 (16.8) Cr 97 (16) I	I 61 (3) SmA
28a	Cr 133 (72) I	I 102 (1.2) SmC
28b	Cr 129 (54) I	I 95 (1.1) SmC
28c	Cr 92 (23) SmC 98 (1.2) I	I 96.4 (0.9) SmC
28d	Cr 59 (26) SmA 96 (1.5) I	I 95.4 (1.6) N & SmA
30	Cr 135 (76) I	-
31	Cr 70 (34) I	I 33 (32) Cr
32	Cr 84 (26) Col_r 95 (2.5) I	I 92 (2.4) Col_r

Imidazolium-based ionic liquid crystalline monomer **27** with I^- as counter ion shows a monotropic SmA phase. The solvent crystallized compound shows three endothermic transitions prior to the isotropic transition at 97 ºC. On cooling mesophase appears at 61 ºC which remains stable down to room temperature. Its shows beautiful texture of SmA phase as shown in figure

13. On second heating mesophase to isotropic transition occurs at 62.4 ºC and on second cooling the smectic phase appears within one degree of super cooling.

The first compound of the dimer series **28a**, symmetrically substituted by two mesogenic groups through central imidazolium moiety, showed only a monotropic SmC phase. The crystalline compound **28a** on heating melts at 133 ºC to the isotropic phase. However, on cooling the smectic phase appears at 102 ºC which is stable down to room temperature. Under the microscope it displays a typical schlieren texture having only four brushes as shown in figure 14. The possibility of a nematic phase was ruled out as the uniaxial nematic phase usually exhibits a schlieren texture with two and four point singularities (two and four brushes). The DSC traces of the compound **28a** is reproduced in figure 15. Compound **28b** also shows monotropic SmC phase. On heating it melts at 129 ºC and phase comes on cooling at 95 ºC which is stable down to room temperature (figure 16). Compounds **28c** exhibits an enantiotropic SmC phase. Upon heating, it melts at about 92 ºC to the SmC phase, which clears at about 98 ºC. On cooling the smectic phase appears within about one degree of super cooling. The compound does not crystallize and the phase remained stable down to room temperature. Under microscope it shows a well defined texture of SmC as shown in figure 17. Compound **28d** exhibits an enantiotropic SmA phase. On heating it melts at about 59 ºC to the SmA phase, which clears at about 96 ºC. On cooling compound **28d** shows N phase at about 95.4 ºC which changes slowly to homeotropic SmA phase as shown in figure 18. The DSC traces of compound **28d** is shown in figure 19. The compound does not crystallize and phase remains stable below room temperature. Compound **30** does not show any liquid crystalline phase. The crystalline compound **30** melts at 135 ºC to the isotropic phase. This could be because of the presence of two incompatible calamitic and discotic groups in the molecule. Similarly, imidazole terminated triphenylene **31**

shows only a crystal to isotropic transition at 70 ºC. On cooling it crystallizes at about 33 ºC. Compound **32** with two triphenylene disk exhibits columnar mesophase. It melts at 84 ºC to the columnar phase which clears at about 95 ºC. On cooling columnar phase appears at 92 ºC. Similar to other samples it does not show any crystallization peak in DSC. The DSC and photomicrograph of the columnar texture is shown in figure 20 & 21 respectively.

5.6 X-ray diffraction studies

The nature of the mesophases was confirmed by X-ray diffraction studies. The diffraction pattern of the SmC phase of calamitic-calamitic hybrid **28b** showed a diffuse peak in the wide angle region with a spacing of about 0.43 nm and corresponds to the average lateral separation of the molecules in this fluid phase. Additionally, a single sharp peak was observed in the small angle region of the diffraction pattern as shown in figure 22. It has a spacing of about 2.7 nm at 40 ºC, which is much lower than the full molecular length. Therefore, the tilt angle of the molecule in the SmC phase is found to be about 47°. In the N phase of compound **28d** a diffuse peak is observed in the small angle region of the diffraction pattern along the field direction, figure 23. It has a spacing of about 1.54 nm at 95 ºC. This spacing is approximately comparable to the rigid aromatic core of the molecule. On the other hand in the SmA phase it shows an additional sharp peak (figure 24) in the small angle region with a spacing of about 3.11 nm at 80 ºC which matches very well with the spacing expected from an intercalated structure as shown in figure 25. This length is approximately same from the middle of imidazolium moiety of one mesogenic unit to the middle of another imidazole moiety of second mesogenic unit. The diffraction pattern of the ionic dimer made from discotic-discotic moiety **32** is shown in figure 26. The sample was heated to the isotropic phase and then cooled to room temperature. The diffraction pattern was

taken at room temperature. In the small angle region, six reflections were observed, which can be indexed (as shown in figure 26) on a simple rectangular lattice of lattice parameter a = 3.48 nm and b = 3.03 nm.

5.7 Conclusion

In conclusion, we have synthesized novel imidazolium-based ionic liquid crystalline dimers based on calamitic-calamitic, calamitic-discotic, discotic-discotic moieties using microwave irradiation. The quaternization of imidazole-substituted mesogens under classical reaction conditions failed to produce the desired quaternary salts. Polarizing optical microscopy and X-ray diffraction experiments showed smectic and columnar phases of the calamitic-calamitic and discotic-discotic hybrids, respectively.

5.8 Ionic discotic liquid crystalline polymers

5.8.1 Synthesis

The ionic polymer **38** was synthesized by the route shown in Scheme 3.

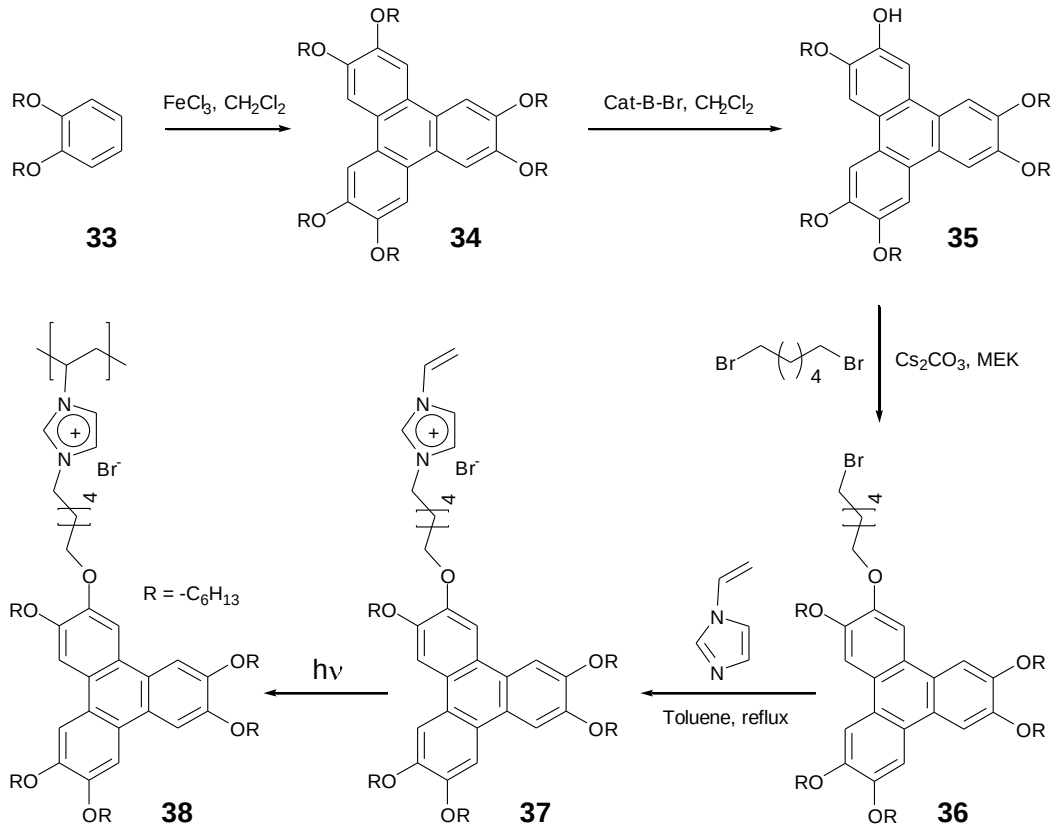

Scheme 3

Hexaalkoxytriphenylene **34**, monohydroxytriphenylenes **35** and ω-bromo-substituted triphenylenes **36** were prepared following literature methods [31]. Thus oxidative trimerization of dialkoxybenzene **33** with $FeCl_3$ in presence of a catalytic amount of H_2SO_4 gives rise to hexaalkoxytriphenylenes **34** in 65 % yield. Selective cleavage of one of the aryl-ether bond of **34** using B-bromocatecholborane furnished monohydroxytriphenylenes **35** in about 50 % yield. Monohydroxytriphenylene on reflux with appropriate dibromide in presence of Cs_2CO_3 as a base and methyl ethyl ketone as a solvent give rise to bromo-terminated triphenylene **36** in about 70

% yield. Liquid crystalline imidazolium salt **37** was obtained by reacting the bromo-substituted compounds **36** with 1-vinylimidazole using toluene as a solvent under nitrogen atmosphere for 48 hours in about 70 % yield. Compound **37** was photopolymerised in presence of 2,2-dimethoxy-2-phenyl acetophenone as the photoinitiator to give **38**. The mixture of photoinitiator and monomer **37** was sandwiched between two glass substrates, heated to an isotropic state at 100°C, and then cooled to room temperature at a cooling rate of 1 °C min^{-1}. Phopolymerization of columnar liquid crystals was carried out under the exposure of UV light for 1 hour.

5.8.2 Characterization

All the compounds were purified by repeated column chromatography followed by crystallization and characterized from their ^{1}H NMR, IR, UV spectra and elemental analysis. Spectral data of all the compounds were in good agreement with their structures indicating high purity of the materials.

The ^{1}H NMR of compound **37** is reproduced in figure 27. As expected from the structure below, Proton H_b is flanked between two strong electronegative nitrogen atoms and therefore, appear at the highest δ value compare to other hydrogens as evident clearly in the NMR spectrum (δ = 11.3 ppm). The triphenylene protons (H_a) appear as a multiplet (m) with a δ value of 7.82 ppm. H_c and H_d protons in the imidazolium moiety resonate at δ 7.30 and 7.21 ppm, respectively. As H_e proton in the vinyl group attached through a central cationic imidazolium moiety it resonates at a higher δ value compare to other two olefinic protons (H_g and H_f) and appear as a quartet (q) at δ 7.37 ppm in the spectrum. Similarly, H_g and H_f resonate at δ values 5.78 and 5.35 ppm, respectively and appear as a quartet. The N^+CH_2 and $–OCH_2$ appear as triplet

and multiplets at δ values 4.43 and 4.24 ppm, respectively. Other aliphatic protons can be clearly seen in between δ 1.0-2.1 ppm. This confirms the structure and high purity of the compound.

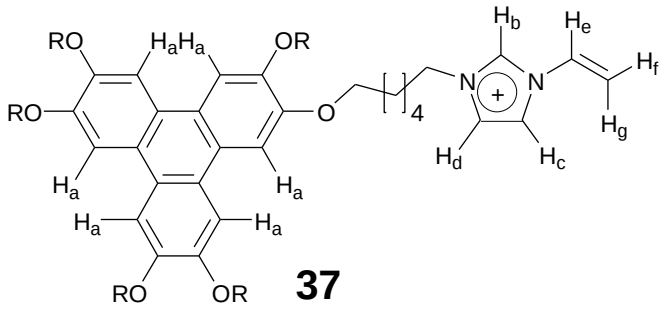

37

Figure 28 represents the ^{1}H NMR spectrum of the polymer **38**. As expected all the peaks becomes broad in nature. The three hydrogens in the imidazolium moiety appear as broad singlet. Similarly, triphenylene hydrogens appear as broad multiplet in the same region as described above. The –OCH_2 protons resonate in the region of δ 3.85-4.30 ppm and appear as broad multiplet. All other aliphatic hydrogens appear in the region of δ 0.8-2.0 ppm.

Gel permeation chromatography (GPC) was taken to characterize the polymer further. The polymer showed a very broad peak near THF signal (figure 29) which corresponds to low molecular weight oligomers. The calculated weight average molecular weight is around 5352 and number average molecular weight is nearly 1192 with respect to polystyrene standard. So polydispersity index in the polymer comes around 4.

5.8.3 Thermal behaviour

Compound **37** exhibited a broad melting peak at 88°C in the first heating run in the DSC. On cooling, a well-defined texture of a columnar mesophase appeared at 75 °C and remained stable down to room temperature. The DSC first cooling run showed the isotropic phase to columnar mesophase peak centered at 72 °C and no other crystallization peak was observed up to room

temperature. During the second heating, the mesophase to isotropic phase transition appeared at 77 °C with a much lower heat of transition indicating a mesophase to isotropic transition. On second cooling, the isotropic phase to columnar mesophase peak again appeared at 72 °C. On the other hand the ionic polymer **38**, which is glassy at room temperature, showed a very broad melting at around 224 °C and finally went to isotropic at 244 °C. On cooling mesophase appeared at around 209 °C and remains stable down to room temperature. However the material was not deformed at room temperature. Probably, it vitrified and formed a stable super cooled glassy columnar phase. Optical microscopy displayed birefringent but undefined texture (figure 30), which is very common in liquid crystalline polymers.

5.8.4 X-ray diffraction studies

The nature of the mesophase was confirmed from X-ray diffraction studies. Compound **37** showed 7 reflections which can be indexed in a simple rectangular lattice with lattice parameter a = 3.68 nm, b = 1.49 nm. In case of polymer the sample was heated to isotropic state and diffraction pattern was recorded at room temperature. Here the lattice parameters were found to be almost same (a = 3.71 nm, b = 1.54 nm) as in the case of monomer, only peaks have broadened. This supports that columnar rectangular lattice is still maintained in the polymer. The X-ray diffraction pattern and intensity *vs.* 2θ of both monomers and polymers have been shown in figure 31.

5.8.5 Conclusion

In conclusion we have prepared and characterized a ionic discotic liquid crystalline polymer based on triphenylene for the first time. X-ray diffraction study indicates the columnar order is

small in polymer compare to monomer. GPC showed that the polymer is actually a mixture of low molecular weight oligomers. This is probably due to steric hindrance of triphenylene units into the side chain. Such ionic discotic polymers are not only important as polymeric molten salts in materials science, but also contribute to the development of novel anisotropic soft materials for directional ion conductivity and charge transport.

5.9 Experimental

5.9.1 General information

General experimental conditions have been described in chapter 2.

5.9.2 Synthesis of alkoxycyanobiphenyl-based imidazolium ionic liquids

Synthesis of compound **25** has been described in chapter 2.

Synthesis of 26: A DMF solution of imidazole (34 mg, 0.5 mmol) in a round-bottomed flask (50 ml) equipped with a stirring bar was deaerated under reduced pressure, and the flask was filled with argon. The deareation was repeated three times to remove oxygen in the flask, thoroughly. The flask was kept in an ice-bath to maintain the temperature of about 0 °C inside. After that 13 mg of NaH (0.55 mmol) was added slowly into the reaction mixture. Then 100 mg of triphenylene bromide (0.25 mmol) was added and the resulting mixture was heated at 70 °C for 2 h with vigorous stirring. After the reaction is over, the mixture was poured into a mixture of ethyl acetate (EtOAc) and water (50 ml). The organic phase was separated; the aqueous phase was extracted with EtOAc three times. The combined organic extracts were washed with water and saturated NaCl solution respectively. The resulting organic phase was dried over anhydrous

sodium sulfate and concentrated under reduced pressure. The residue was purified through a small silica column (3-5 % ethyl acetate) to give pure product (52 mg, 50 %).

^{1}H NMR (400 MHz, $CDCl_3$): δ 7.66 (d, 2H), 7.63 (d, 2H), 7.53 (d, 2H), 7.48 (s, 1H), 7.10 (s, 1H), 6.99 (d, 2H), 6.93 (s, 1H), 4.00 (t, 2H), 3.93 (t, 2H), 1.2-1.8 (m, 14H).

Elemental analysis: calculated for $C_{25}H_{29}ON_3$, C 77.48, H 7.54, N 10.84 %; found C 76.90, H 7.31, N 10.72 %.

Synthesis of 27: Compound **26** (100 mg) was taken in a round-bottomed flask (50 ml) and excess of MeI (2 ml) was added to it. The mixture was stirred at room temperature for 24 hours under N_2. After the reaction is over, the mixture was kept in high vacuum to remove excess of methyl iodide and the product was recrystalised from dry diethyl ether two times to get the quaternized product (100 mg, 75 % yield).

^{1}H NMR (400 MHz, $CDCl_3$): δ 10.1 (s, 1H), 7.69 (d, 2H), 7.64 (d, 2H), 7.53 (d, 2H), 7.22 (s, 2H), 6.99 (d, 2H), 4.29 (t, 2H), 4.1 (s, 3H), 4.00 (t, 2H), 1.3-1.9 (m, 14H).

Elemental analysis: calculated for $C_{26}H_{32}OBrN_3$, C 64.73, H 6.69, N 8.71 %; found C 65.0, H 5.59, N 8.70 %.

Synthesis of 28a: In a typical reaction, **26** (20 mg, 0.052 mmol), **25** (22.7mg, 0.057 mmol) were mixed in 1-methyl-pyrrolidinone (0.2 ml) in a small glass vial and loosely covered with a rubber septum. The mixture was heated in an unmodified household microwave oven at 360 W for 1 minute. The vial was taken out and water (2 ml) was added and centrifuged at 5000 rpm for 1 hour. The supernatant liquid was removed and white solid was recrystalised two times from acetone to furnished **28a** (20 mg, 50 %).

28a: **^{1}H NMR** (400 MHz, $CDCl_3$): δ 10.72 (s, 1H), 7.64 (d, *J* = 8.3 Hz, 4H), 7.59 (d, *J* = 8.3 Hz, 4H), 7.48 (d, *J* = 8.7 Hz, 4H), 7.26 (s, 2H), 6.94 (d, *J* = 8.7 Hz, 4H), 4.32 (t, *J* = 7.4 Hz, 4H), 3.96 (t, *J* = 6.4 Hz, 4H) 1.2-2.1 (m, 28H).

IR (KBr, all the derivatives **28a-28d** show similar spectrum): ν_{max} 2952.5, 2925.8, 2225.7, 1602, 1570.6, 1562.2, 1523.2, 1396.4, 1292.2, 1253.6, 1267.1, 1180.4, 1114.8, 1029.9, 852.5, 725.2, 659.6, 532.3 cm^{-1}.

UV-Vis ($CHCl_3$, all the derivatives **28a-28d** show similar spectrum): λ_{max} 307.6 nm.

Elemental analysis: calculated for $C_{47}H_{55}N_4O_2Br$**,** C 71.65, H 7.04, N 7.11 %; found C 71.2, H 7.28, N 7.55 %.

28b: **^{1}H NMR** (400 MHz, $CDCl_3$): δ 11.10 (s, 1H), 7.73 (d, *J* = 8.3 Hz, 4H), 7.62 (d, *J* = 8.3 Hz, 4H), 7.53 (d, *J* = 8.7 Hz, 4H), 7.17 (s, 2H), 6.94 (d, *J* = 8.7 Hz, 4H), 4.53 (t, *J* = 7.4 Hz, 2H), 4.33 (t, *J* = 7.4 Hz, 2H), 4.10 (t, *J* = 6.4 Hz, 2H), 3.99 (t, *J* = 6.4 Hz, 2H), 1.2-2.3 (m, 18H).

Elemental analysis: calculated for $C_{42}H_{45}N_4O_2Br$**,** C 70.29, H 6.29, N 7.81 %; found C 70.03, H 5.77, N 7.96 %.

28c: **^{1}H NMR** (400 MHz, $CDCl_3$): δ 10.95 (s, 1H), 7.69 (d, *J* = 8.3 Hz, 4H), 7.63 (d, *J* = 8.3 Hz, 4H), 7.53 (d, *J* = 8.7 Hz, 4H), 7.19 (s, 1H), 7.17 (s, 1H), 6.99 (d, *J* = 8.7 Hz, 4H), 4.40 (t, *J* = 7.4 Hz, 2H), 4.36 (t, *J* = 7.4 Hz, 2H), 3.95-4.05 (m, 4H), 1.3-2.1 (m, 24H).

Elemental analysis: calculated for $C_{44}H_{49}N_4O_2Br$**,** C 70.8, H 6.62, N 7.52 %; found C 70.53, H 6.94, N 7.76 %.

28d: **^{1}H NMR** (400 MHz, $CDCl_3$): δ 10.95 (s, 1H), 7.69 (d, *J* = 8.3 Hz, 4H), 7.63 (d, *J* = 8.3 Hz, 4H), 7.53 (d, *J* = 8.7 Hz, 4H), 7.17 (s, 2H), 6.99 (d, *J* = 8.7 Hz, 4H), 4.32-4.39 (m, 4H), 4.00 (m, 4H), 1.2-2.0 (m, 30H).

Elemental analysis: calculated for $C_{48}H_{57}N_4O_2Br$**,** C 71.9, H 7.11, N 6.99 %; found C 71.5, H 7.28, N 6.90 %.

5.9.3 Synthesis of imidazolium-based calamitic-discotic ionic dimers

The synthesis of **29** has been described elsewhere [31].

Synthesis of 30: In a typical reaction, **26** (20 mg, 0.052 mmol), **29** (46.7mg, 0.062 mmol) were mixed in 1-methyl-pyrrolidinone (0.2 ml) in a small glass vial and loosely covered with a rubber septum. The mixture was heated in an unmodified household microwave oven at 360 W for 1 minute. The vial was taken out and water (2 ml) was added and centrifuged at 5000 rpm for 1 hour. The supernatant liquid was removed and white solid was recrystalised two times from acetone to furnished **30** (28 mg, 50 %).

30: ^{1}H NMR (400 MHz, $CDCl_3$): δ 10.85 (s, 1H), 7.81-7.83 (m, 6H), 7.68 (d, *J* = 8.3 Hz, 2H), 7.62 (d, *J* = 8.3 Hz, 2H), 7.51 (d, *J* = 8.6 Hz, 2H), 7.24 (s, 1H), 7.09 (s, 1H), 6.96 (d, *J* = 8.7 Hz, 2H), 4.45 (t, *J* = 7.2 Hz, 2H), 4.29 (t, *J* = 7.2 Hz, 2H), 4.25 (m, 12H), 3.95 (t, *J* = 6.4 Hz, 2H), 1.0-2.1 (m, 55H).

IR (KBr): 2923.9, 2854.5, 1618.2, 1612.4, 1560.3, 1544.9, 1460, 1377.1, 1261.4, 1172.6, 1070.4, 1033.8, 835.1, 771.5, 721.3, 667.3.

UV-Vis ($CHCl_3$): λ_{max} 305.2, 278, 265, 347.2 nm.

Elemental analysis: calculated for $C_{68}H_{90}N_3O_7Br$**,** C 71.56, H 7.95, N 3.68 %; found C 71.1, H 7.95, N 4.08 %.

5.9.4 Synthesis of imidazolium-based discotic-discotic ionic dimers

Synthesis of 31: The synthesis **31** has been described in chapter 4.

Synthesis of 32: In a typical reaction, **31** (20 mg, 0.026 mmol), **29** (24.4 mg, 0.032 mmol) were mixed in 1-methyl-pyrrolidinone (0.2 ml) in a small glass vial and loosely covered with a rubber septum. The mixture was heated in an unmodified household microwave oven at 360 W for 1 minute. The vial was taken out and water (2 ml) was added and centrifuged at 5000 rpm for 1 hour. The supernatant liquid was removed and white solid was recrystalised two times from acetone to furnished **32** (19.9 mg, 50 %).

32: ^{1}H NMR (400 MHz, $CDCl_3$): δ 10.77 (s, 1H), 7.80-7.82 (m, 12H), 7.19 (s, 2H), 4.40 (t, *J* = 7.3 Hz, 4H), 4.23 (m, 24H), 1.2-2.1 (m, 82H).

IR (KBr): 2923.9, 2854.5, 1618.2, 1612.4, 1560.3, 1544.9, 1460, 1377.1, 1261.4, 1172.6, 1070.4, 1033.8, 835.1, 771.5, 721.3, 667.3.

UV-Vis ($CHCl_3$): λ_{max} 344.4, 305.2, 278.2, 269.6, 259 nm.

Elemental analysis: calculated for $C_{89}H_{125}N_2O_{12}Br$**,** C 71.51, H 8.43, N 1.87 %; found C 71.1, H 8.45, N 2.15 %.

5.9.5 Synthesis of imidazolium-based ionic discotic polymer

The synthesis of **33**, **34**, **35**, **36** has been described elsewhere [31].

Synthesis of **37:** In a round bottom flask, 0.1 g of compound **36** was dissolved in 2.5 ml of toluene. To this, 2 ml of 1-vinyl imidazole was added and the reaction mixture was heated at 80 °C for 48 hours under nitrogen with stirring. The solvent and excess of 1-vinyl imidazole were removed under vacuum and the residue was recrystallized twice from dry diethyl ether to afford the quaternized product **37** (80 mg, 71 %).

^{1}H NMR (400 MHz, $CDCl_3$): δ 11.3 (s, 1H), 7.82 (m, 6H), 7.37 (q, 1H), 7.30 (s, 1H), 7.21 (s, 1H), 5.78 (dd, 1H), 5.35 (dd, 1H), 4.43 (t, 2H), 4.24 (m, 6H), 1.02-2.03 (m, 49H).

Elemental analysis: calculated for $C_{49}H_{69}O_6N_2Br$, C 68.29, H 8.06, N 3.25 %; found C 67.89, H 8.08, N 3.99 %.

Synthesis of 38: The polymerizable sample (**38**) was prepared by mixing monomer **37** and 2,2-dimethoxy-2-phenylacetophenone (5 wt % to the monomer) as the photoinitiator. The mixture was sandwiched between two glass substrates, heated to an isotropic state at 100°C, and then cooled to room temperature at a cooling rate of 1°C min^{-1}. Polymerization of columnar liquid crystals was carried out under the exposure of UV light (400 W).

^{1}H NMR (400 MHz, $CDCl_3$, b represents broad peak): δ 11.4 (s, b), 7.8 (m, b), 7.53 (s, b), 7.0 (s, b), 3.85-4.30 (m, b), 0.8-2.0 (m, b).

References

[1] C. Tschierske, *J. Mater. Chem*., **8**, 1485 (1998).

[2] F. Neve, *Adv. Mater*., **8**, 277 (1996).

[3] M. Veber, G. Berruyer, *Liq. Cryst*., **27**, 671 (2000).

[4] (a) M. Veber, C. Jallabert, H. Strzelecka, V. Gionis, G. Sigaud, *Mol. Cryst. Liq. Cryst*., **137**, 373 (1986). (b) H. Strzelecka, C. Jallabert, M. Veber, *Mol. Cryst. Liq. Cryst*., **156**, 355 (1988). (c) P. Davison, C. Jallabert, A. M. Levelut, H. Strzelecka, M. Veber, *Liq. Cryst*., **3**, 133 (1988). (d) M. Veber, C. Jallabert, H. Strzelecka, *Synth. Comm*., **17**, 693 (1987). (e) M. Veber, C. Jallabert, H. Strzelecka, O. Jullien, P. Davidson, *Liq. Cryst*., **8**, 775 (1990).

[5] D. W. Bruce, *Acc. Chem. Res*., **33**, 831 (2000).

[6] D. W. Bruce, S. A. Hudson, *J. Mater. Chem*., **4**, 479 (1994).

[7] B. Donnio, D. W. Bruce, *New J. Chem*., 275 (1999).

[8] M. Marcos, M. B. Ros, J. L. Serrano, M. A. Esteruelas, E. Sola, L. A. Oro, J. Barbera, *Chem. Mater*., **2**, 748 (1990).

[9] D. M. Huck, H. C. Nguyen, B. Donnio, D. W. Bruce, *Liq. Cryst*., **31**, 503 (2004).

[10] (a) ‘’*Liquid Crystalline Order in polymers*’’, ed. A. Blumstein, Acadenic prerss, New York, (1978). (b) ‘’polymer Liquid Crystals’’, in *‘’Materials Science and Technology series’’*, ed. A. Ciferri, W. R. Krigbaum, R. B. Meyer, Academic Press, New York, (1982).

[11] (a) Y. Xue, M. Hara, *Macromolecules*, **30**, 3803 (1997). (b) Y. Xue, M. Hara, H. N. Yoon, *Macromolecules*, **31**, 7806 (1998). (c) Y. Xue, M. Hara, H. N. Yoon, *Macromolecules*, **34**, 844 (2001).

[12] C. M, Paleos, G. Margomenou-Leonidopoulou, C. Christias, *Mol. Cryst. Liq. Cryst*., **137**, 391 (1986).

[13] H. Han, P. K. Bhowmik, *Trends Polym. Sci*., **3**, 199 (1995). (b) P. K. Bhowmik, S. Akhter, H. Han, *J. Polym. Sci. A*, **33**, 1927 (1995). (c) P. K. Bhowmik, W. H. Xu, H. Han, *J. Polym. Sci. A*, **32**, 3205 (1995). (d) P. K. Bhowmik, H. Han, *J. Polym. Sci. A*, **33**, 1745 (1995).

[14] P. K. Bhowmik, H. Han, J. J. Cebe, I. K. Nedeltchev, S. W. Kang, S. Kumar, *Macromolecules*, **37**, 2688 (2004).

[15] P. Y. Vuillaume, C. G. Bazuin, J. –C, Galin, *Macromolecules*, **34**, 781 (2000).

[16] A large number of papers have appeared on thermotropic ionic liquid crystals. It is difficult to cover all these and, therefore, only a few selected references are given here. (a) K. binnemans, *Chem. Rev.*, **105**, 4148 (2005). (b) A. Skoulios, *Adv. Coll. Interface Sci.*, **1**, 79 (1967). (c) D. W. Bruce, D. A. Dunmur, E. Lalinde, P. M. Maitlis, P. Styring, *Nature*, **323**, 791 (1986). (d) M. Marcos, M. B. Ros, J. L. Serrano, M. A. Esteruelas, E. Sola, L. A. Oro, J. Barbera, *Chem. Mater*., **2**, 748 (1990). (e) E. Bravo-Grimaldo, D. Navarro-Rodriguez, A. Skoulios, D. Guillon, *Liq. Cryst.*, **20**, 393 (1996). (f) H. Bernhardt, W. Weissflog, H. Kresse, *Liq. Cryst.*, **24**, 895 (1998). (g) C. M. Gordon, J. D. Holbrey, A. R. Kennedy, K. R. Seddon, *J. Mater. Chem.*, **8**, 2627 (1998). (h) D. Tsiourvas, D. Kardassi, C. M. Paleos, A. Skoulios, *Liq. Cryst.*, **27**, 1213 (1998). (i) J. D. Holbrey, K. R. Seddon, *J. Chem. Soc. Dalton Trans.*, 2133 (1999). (j) L. Cui, V. Sapagovas, G. Lattermann, *Liq. Cryst.*, **29**, 1121 (2002). (k) J. De Roche, C. M. Gordon, C. T. Imrie, M. D. Ingram, A. R. Kennedy, F. L. Celso, A. Triolo, *Chem. Mater.*, **15**, 3089 (2003). (l) P. K. Bhowmik, H. Han, I. K. Nedeltchev, J. J. Cebe, *Mol. Cryst. Liq.*

Cryst., **419**, 27 (2004). (m) D. Haristoy, D. Tsiourvas, *Liq. Cryst.*, **31**, 687 (2004). (n) M. Yoshio, T. Kato, T. Mukai, M. Yoshizawa, H. Ohno, *Mol. Cryst. Liq. Cryst.*, **413**, 99 (2004).

[17] (a) P. Y. Vuillaune, C. G, Bazuin, J.-C, Galin, *Macromolecules*, **33**, 781 (2000). (b) P. Y. Vuillaune, J.-C, Galin, C. G, Bazuin, *Macromolecules*, **34**, 859 (2001).

[18] Y. Haramoto, Y. Kusakabe, S. Ujiie, S. Mang, C. Schwarzwalder, A. B. Holmes, *Liq. Cryst*., **27**, 1393 (2000).

[19] Y. Zhao, H. L. Lei, *Macromolecules*, **27**, 4525 (1994). (b) P. Roche, Y. Zhao, *Macromolecules*, **28**, 2819 (1995).

[20] V. Percec, G. Johansson, R. Rodenhouse, *Macromolecules,* **25**, 2563 (1992).

[21] E. B. Barmatov, D. Pebalk, M. Barmatova, V. Shibaev, *Macromol. Rapid Commun*., **21**, 369 (2000). (b) E. B Barmatov, D. A. Pebalk, Barmatova, M. V, V. B. Shibaev, *Polym. Sci. A*, **43**, 44 (2001).

[22] D. Navarro-Rodriguez, D. Gullion, A. Skoulios, Y. Frere, P. Gramain, *Makromol. Chem*., **193**, 3117 (1992). (b) D. Navarro-Rodriguez, Y. Frere, P. Gramain, *Makromol. Chem*., **192**, 2975 (1991).

[23] P. Masson, B. Heinrich, Y. Frere, P. Gramain, *Makromol. Chem*., **195**, 1199 (1994). (b) P. Masson, P. Gramain, D. Gullion, *Makromol. Chem. Phys.*, **196**, 1199 (1995).

[24] (a) W. Kreuder, H. Ringsdorf, *Makromol. Chem. Rapid Commun*., **4**, 807 (1983). (b) W. Kreuder, H. Ringsdorf, P. Tschirner, *Makromol. Chem. Rapid Commun*., **6**, 367 (1985).

[25] (a) H. Ringsdorf, R. Wustefeld, E. Zerta, M. Ebert, J. H. Wendorff, *Angew. Chem. Int. Ed*., **28**, 914 (1989). (b) M. Werth, H. W. Spiess, *Makromol. Chem. Rapid. Commun*., **14**,

329 (1993). (c) D. Stewart, G. S. McHattie, C. Y. Imrie, *J. Mater. Chem*., **8**, 47 (1998). (d) N. Boden, R. J. Bushby, Z. B. Lu, *Liq. Cryst*., **25**, 47 (1998).

[26] C. T. Imrie, R. T Inkster, Z. Lu, M. D. Ingram, *Mol. Cryst. Liq. Cryst*., **408**, 33 (2004).

[27] I. G. Voigt-Martin, R. W. Garbella, P. Schuhmacher, *Macromolecules*, **25**, 961 (1992).

[28] S. Kumar, *Liq. Cryst*., **32**, 1089 (2005).

[29] G. S. Attard, R. W. Date, C. T. Imrie, G. R. Luckhurst, S. J. Roskilly, J. Seddon, L. Taylor, *Liq. Cryst*., **16**, 529 (1994).

[30] N. Boden, R. J. Bushby, P. S. Martin, *Langmuir*, **15**, 3790 (1999).

[31] (a) S. Kumar, M. Manickam, *Chem. Commun*., 1615 (1997). (b) S. Kumar, M. Manickam, *Synthesis*, 1119 (1998). (c) S. Kumar, J. J. Naidu, S. K. Varshney, *Mol. Cryst. Liq. Cryst.*, **411**, 355 (2004). (d) S. K. Pal, H. K. Bisoyi, S. Kumar, *Tetrahedron*, **63**, 6874 (2007).

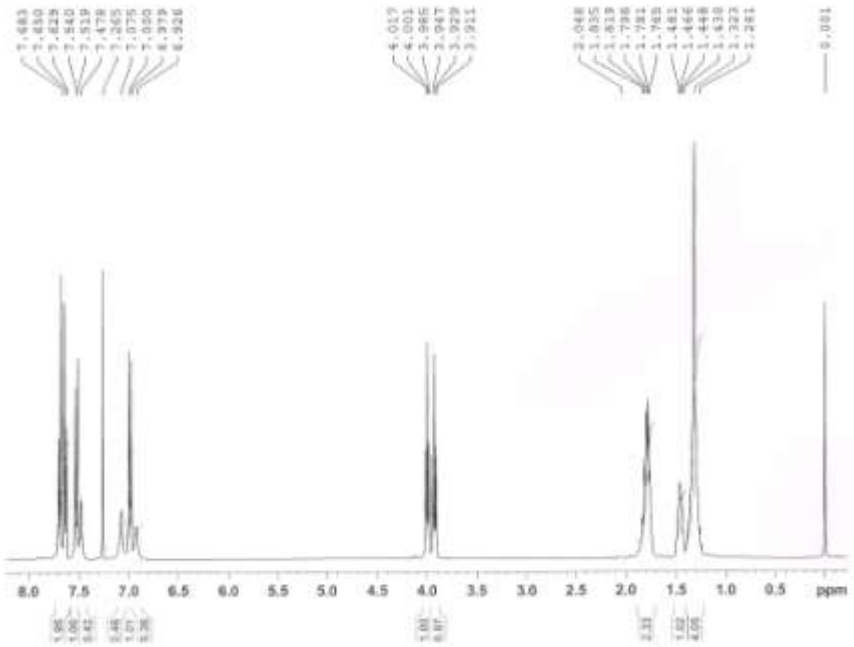

Figure 1. ^{1}H NMR spectrum of the compound **26**.

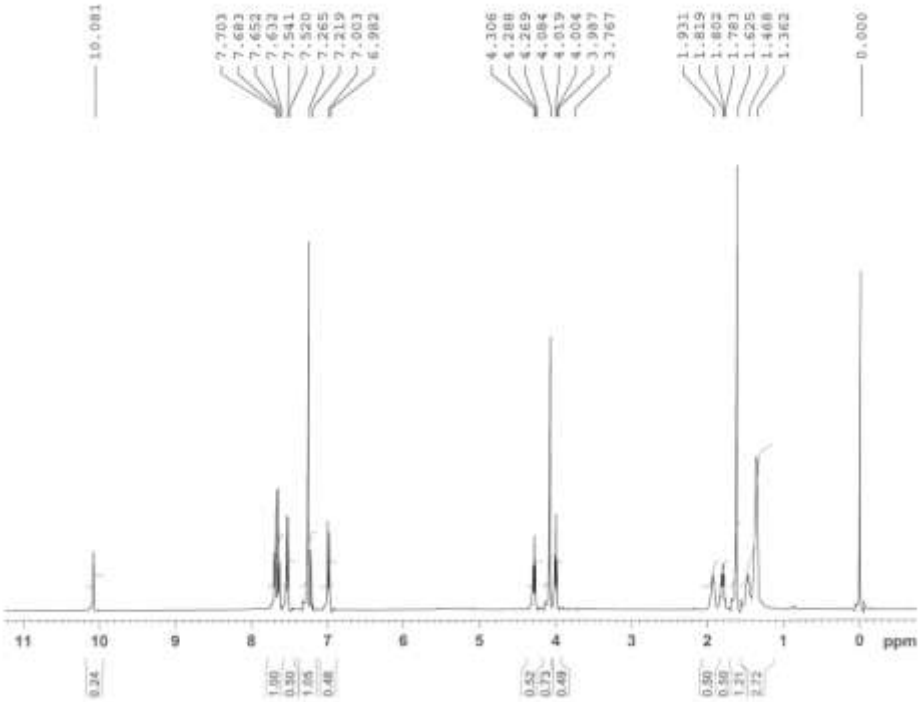

Figure 2. ^{1}H NMR spectrum of the compound **27**.

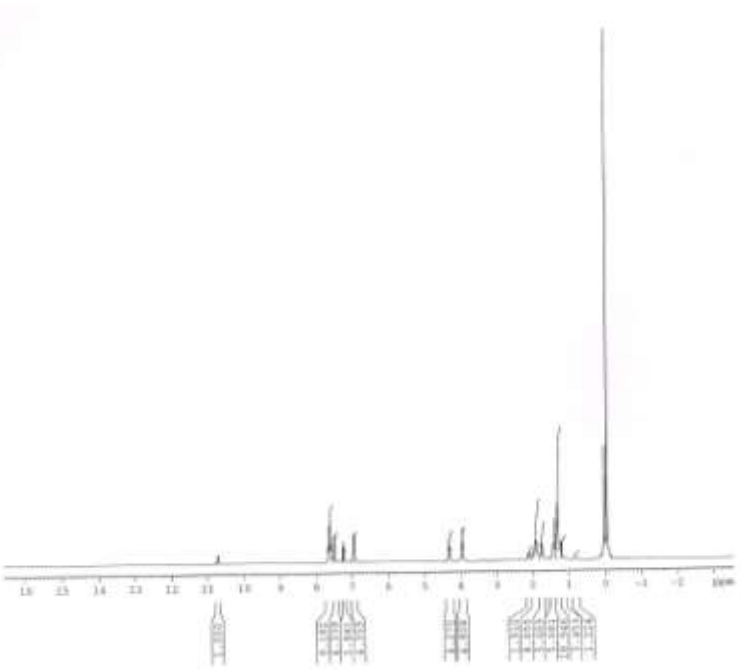

Figure 3. ^{1}H NMR spectrum of the compound **28a**.

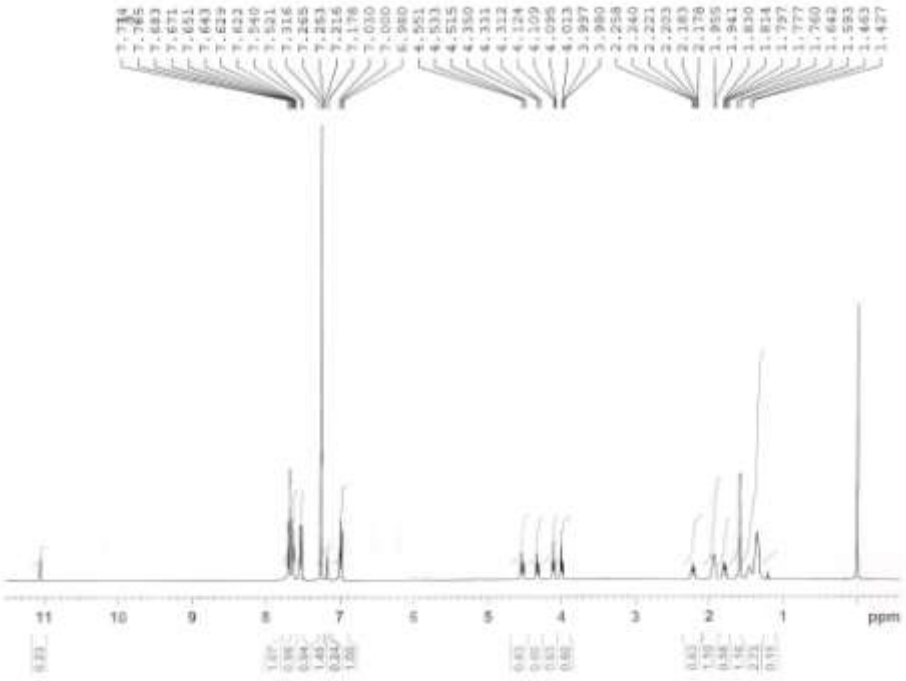

Figure 4. ^{1}H NMR spectrum of the compound **28b**.

Figure 5. IR spectrum of the compound **28a**.

Figure 6. UV spectrum of the compound **28a**.

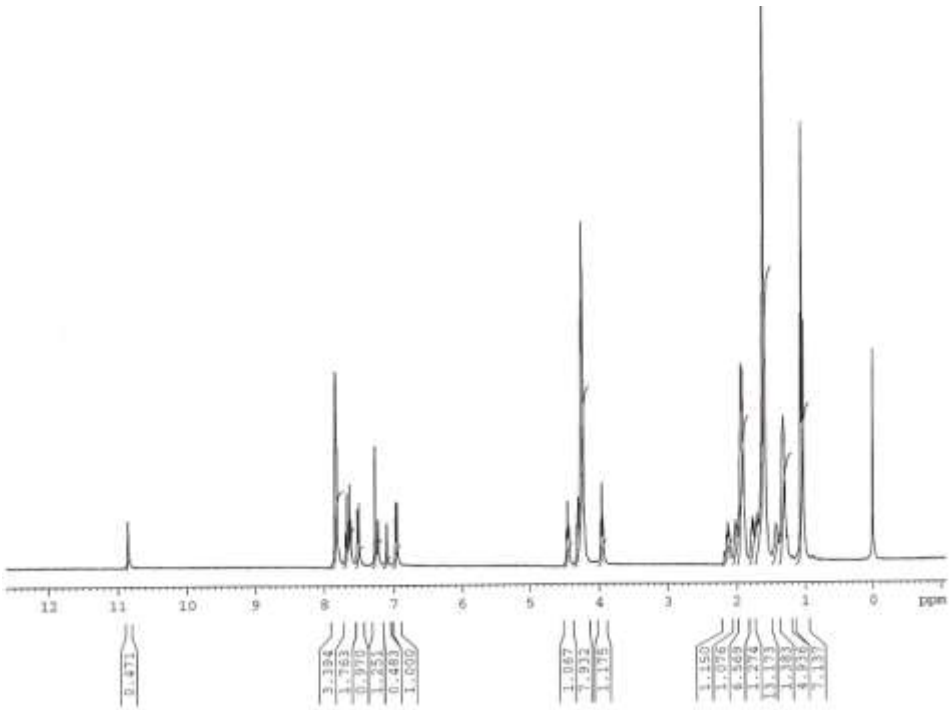

Figure 7. ^{1}H NMR spectrum of the compound **30**.

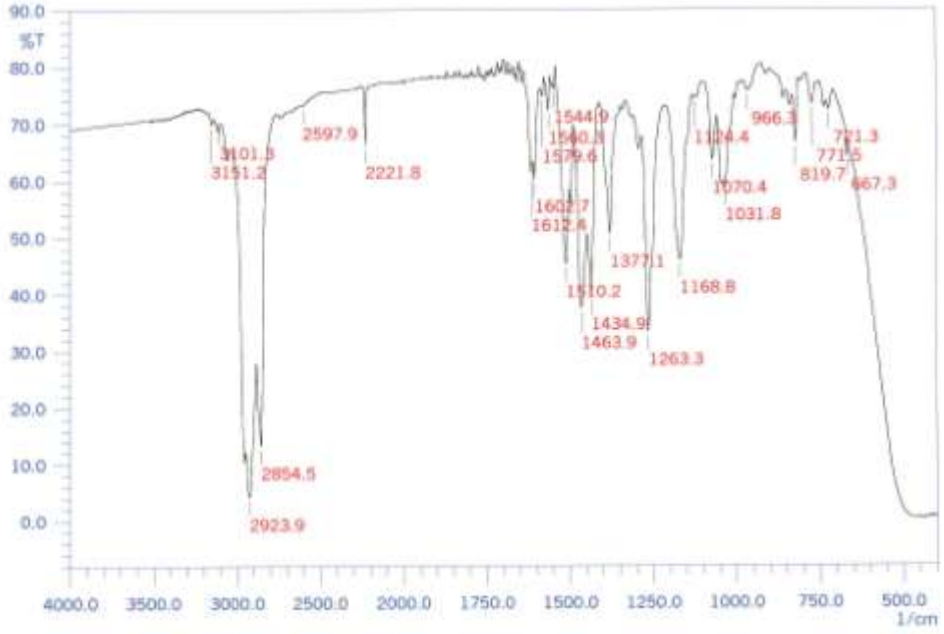

Figure 8. IR spectrum of the compound **30**.

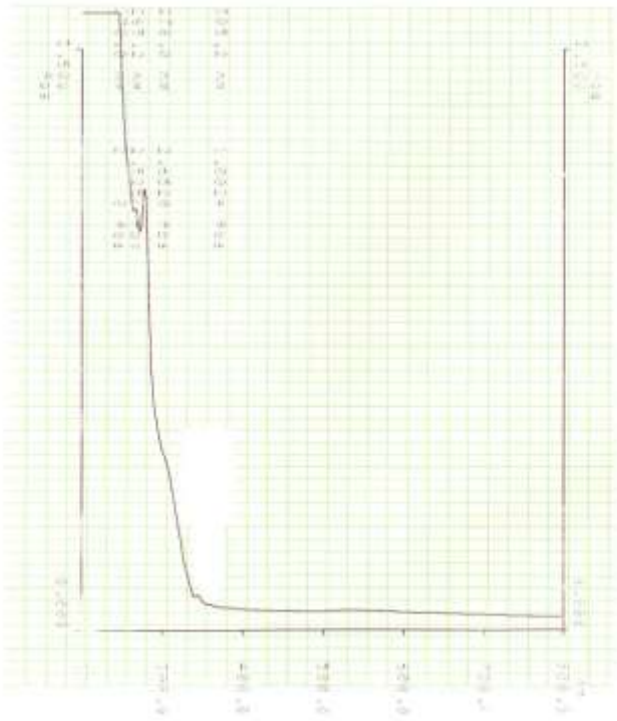

Figure 9. UV spectrum of the compound **30**.

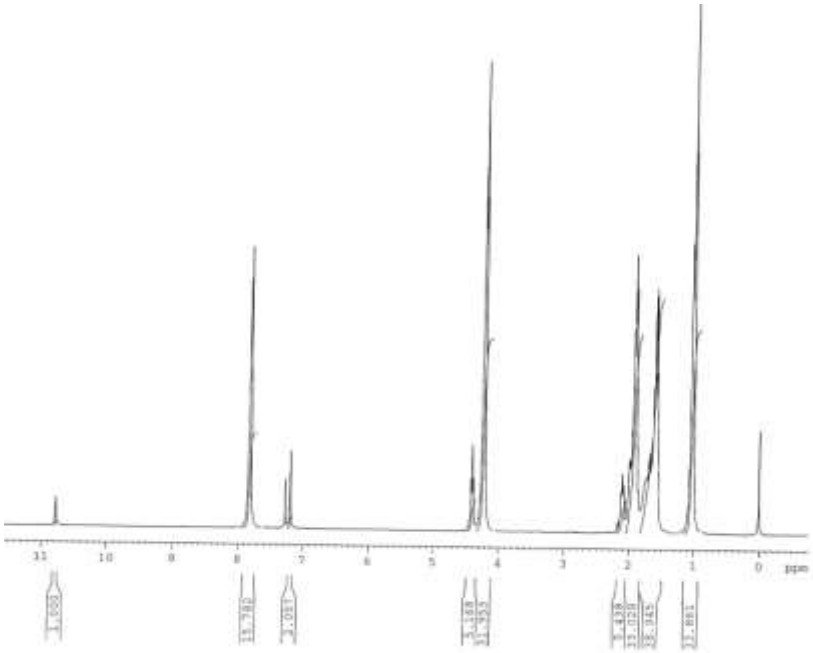

Figure 10. ^{1}H NMR spectrum of the compound **32**.

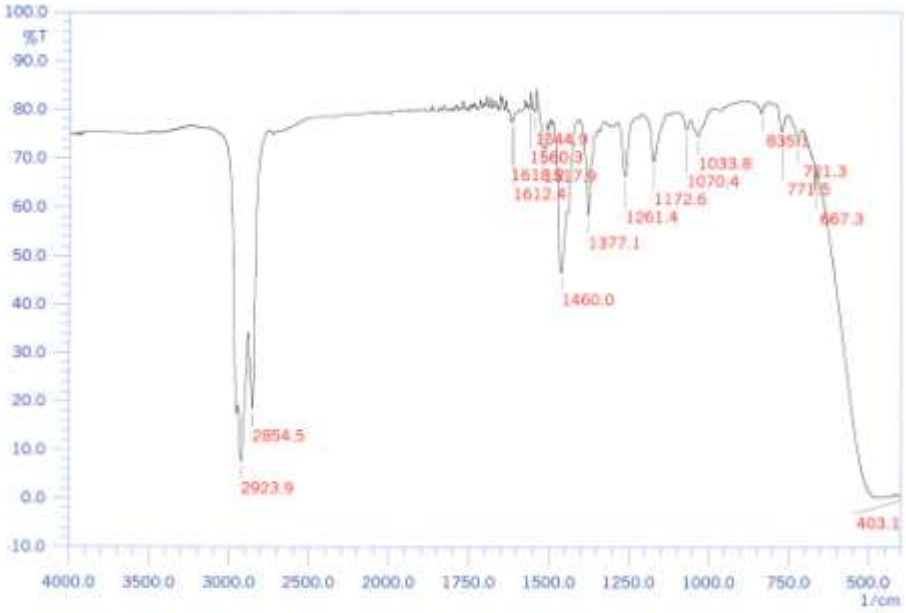

Figure 11. IR spectrum of the compound **32**.

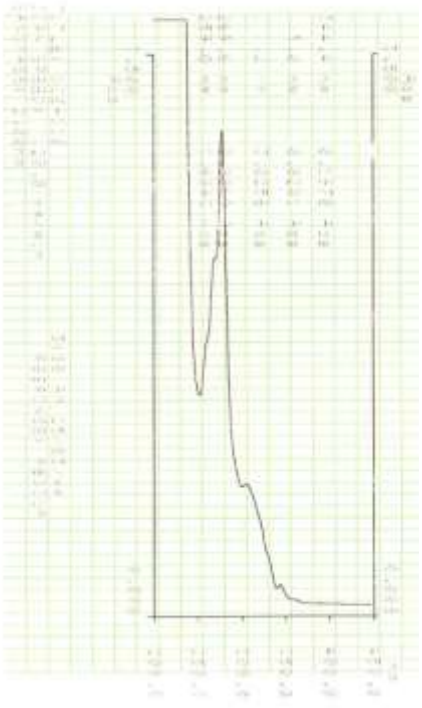

Figure 12. UV spectrum of the compound **32**.

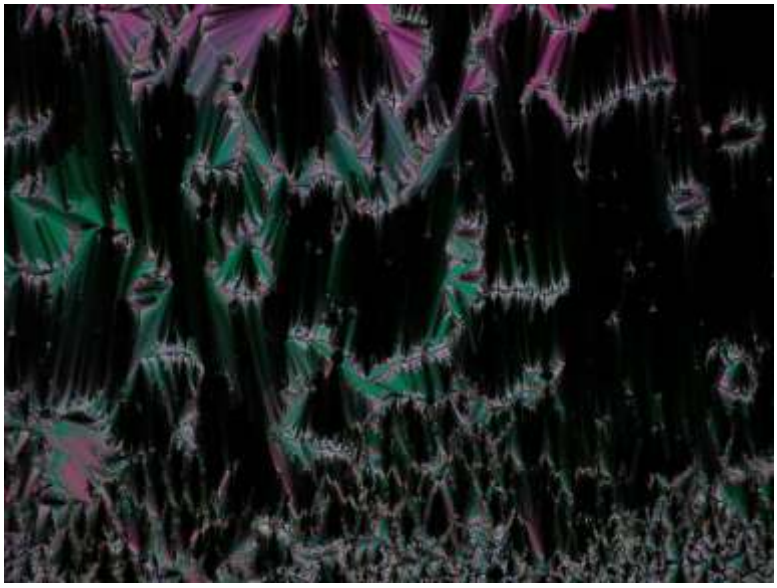

Figure 13. Optical photomicrograph of SmA phase of compound **27** at 50 ºC on cooling from isotropic liquid (Crossed polarizers, magnification X 200).

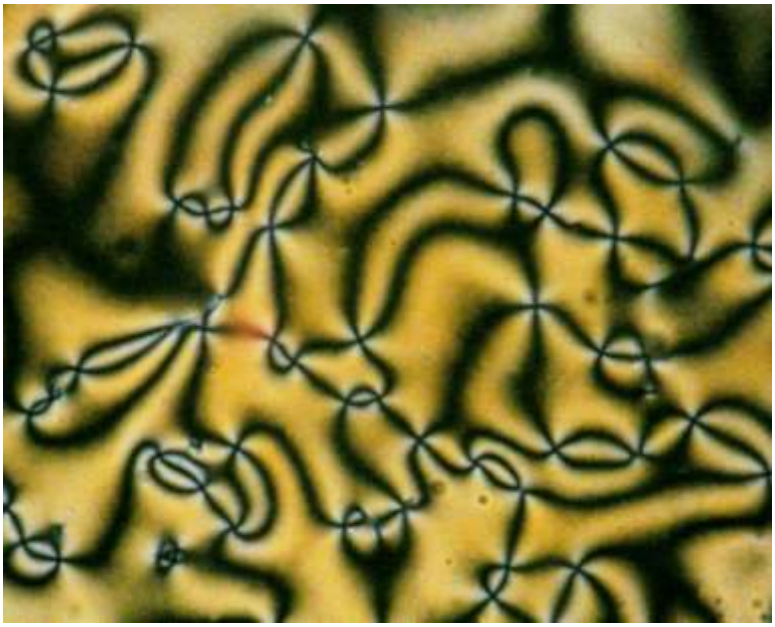

Figure 14. Optical photomicrograph of compound **28a** at 90 ºC on cooling from isotropic liquid (Crossed polarizers, magnification X 200).

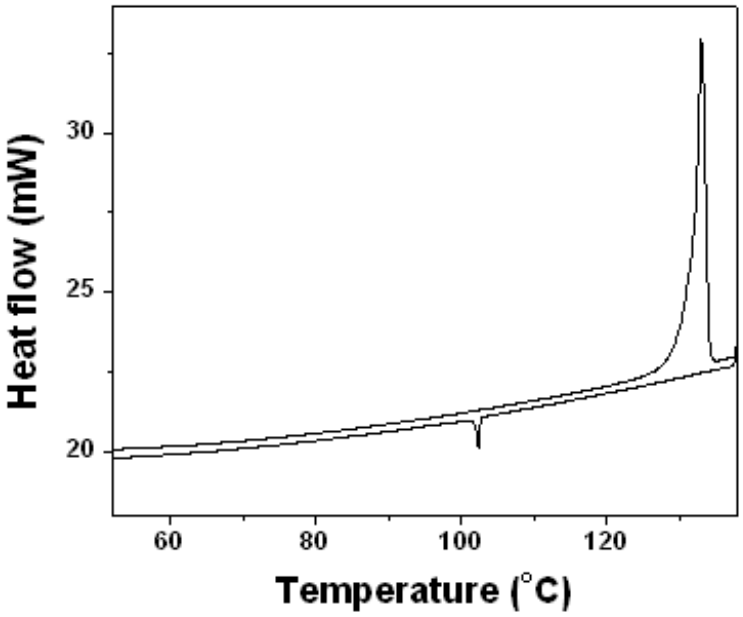

Figure 15. DSC traces of compound **28a** on heating and cooling (scan rate 5 °C/min)

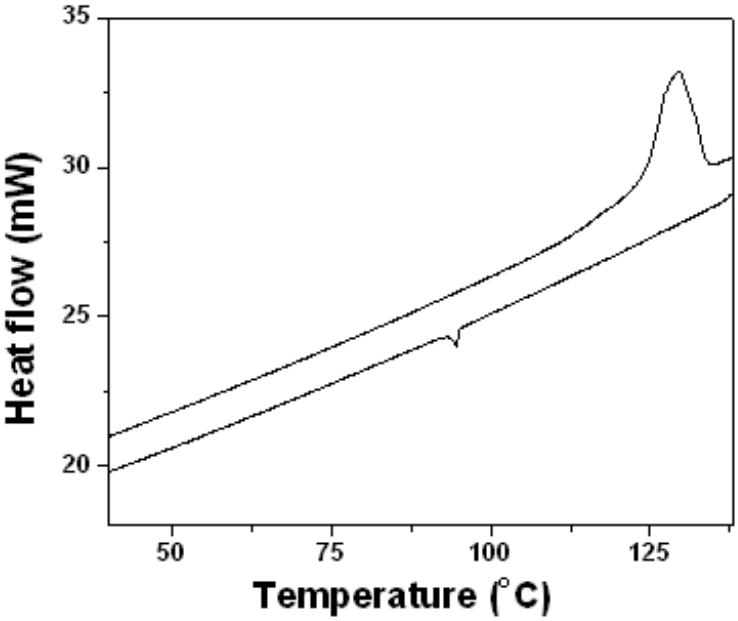

Figure 16. DSC traces of compound **28b** on heating and cooling (scan rate 5 °C/min).

Figure 17. Optical photomicrograph of compound **28c** at 90 ºC on cooling from isotropic liquid (Crossed polarizers, magnification X 200).

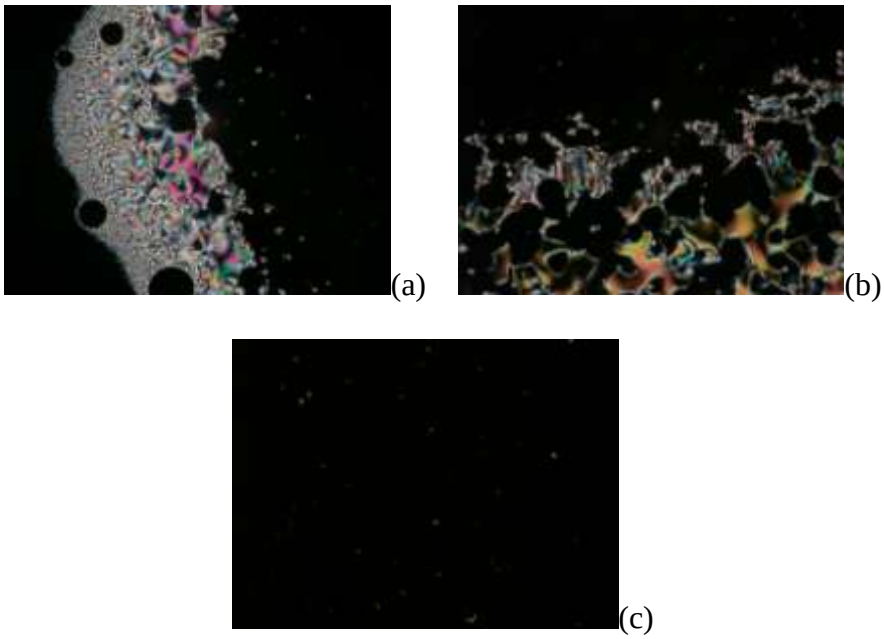

Figure 18. Optical photomicrograph of compound **28d** on cooling from isotropic liquid (a) at 95 °C, N phase (b) at 90 °C, coexistence of N and SmA phase and (c) at 80 °C, homeotropic SmA phase (Crossed polarizers, magnification X 200).

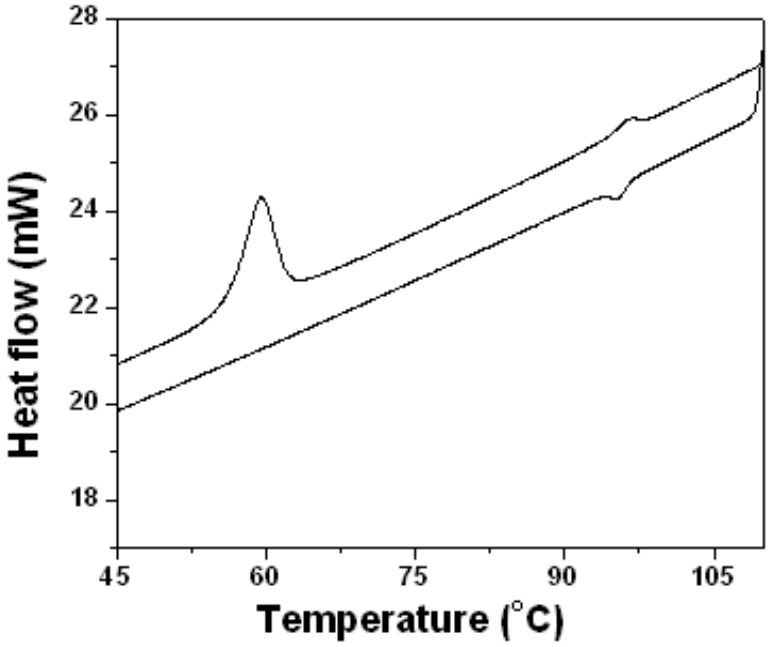

Figure 19. DSC traces of the compound **28d** on heating and cooling (5 °C/ min).

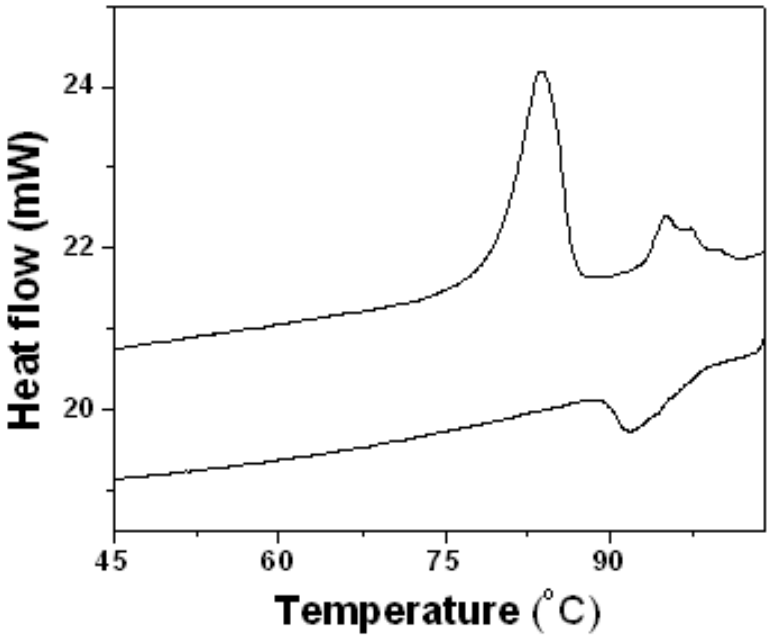

Figure 20. DSC traces of the compound **32** on heating and cooling (5 °C/ min).

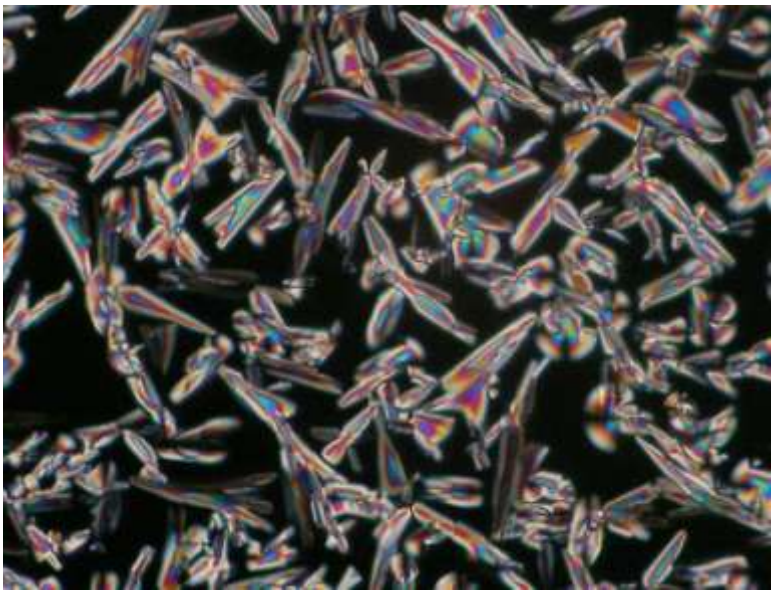

Figure 21. Photomicrograph of the texture of the columnar phase of dimer **32** at 90 °C on cooling from isotropic liquid (Crossed polarizers, magnification X 200).

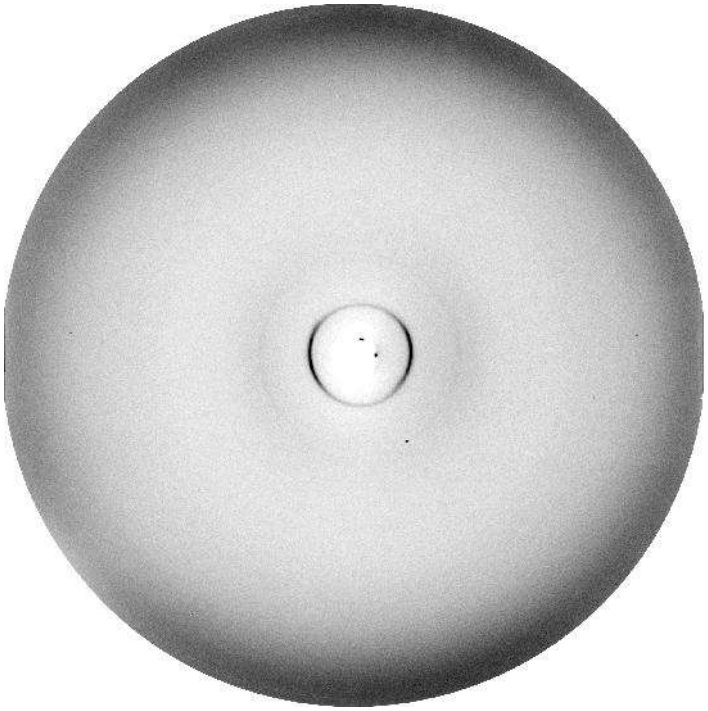

Figure 22. X-ray diffraction pattern obtained for compound **28b** at 90 °C.

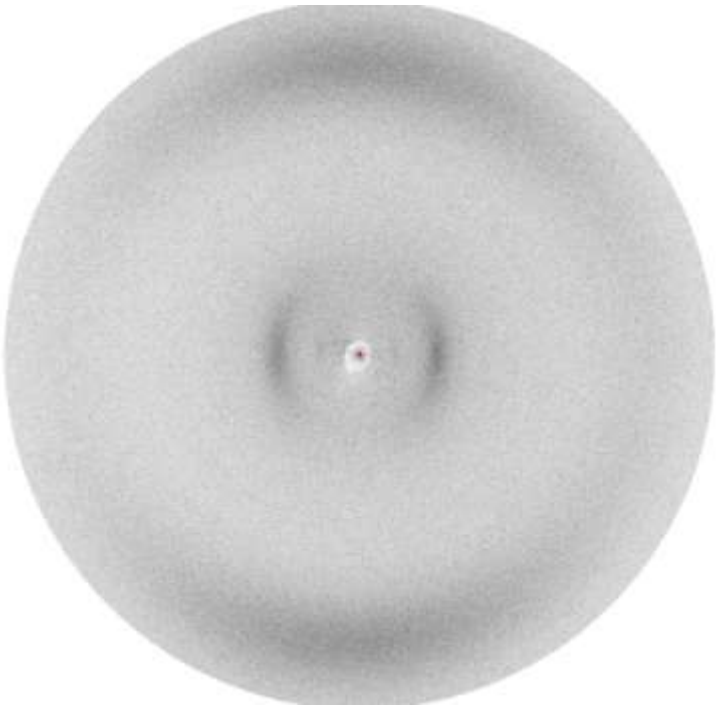

Figure 23. X-ray diffraction pattern obtained for compound **28d** in the N phase at 95 °C.

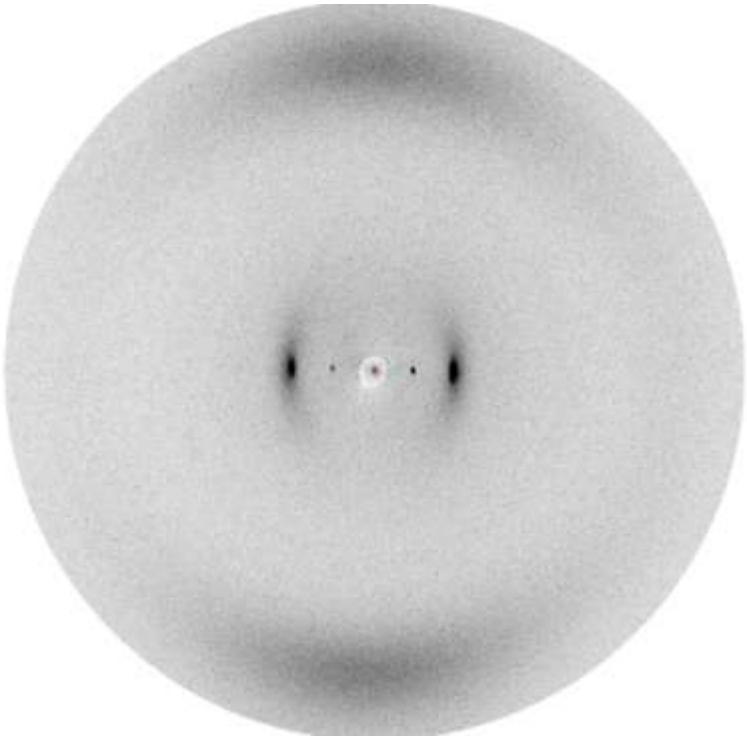

Figure 24. X-ray diffraction pattern obtained for compound **28d** in the SmA phase at 80 °C.

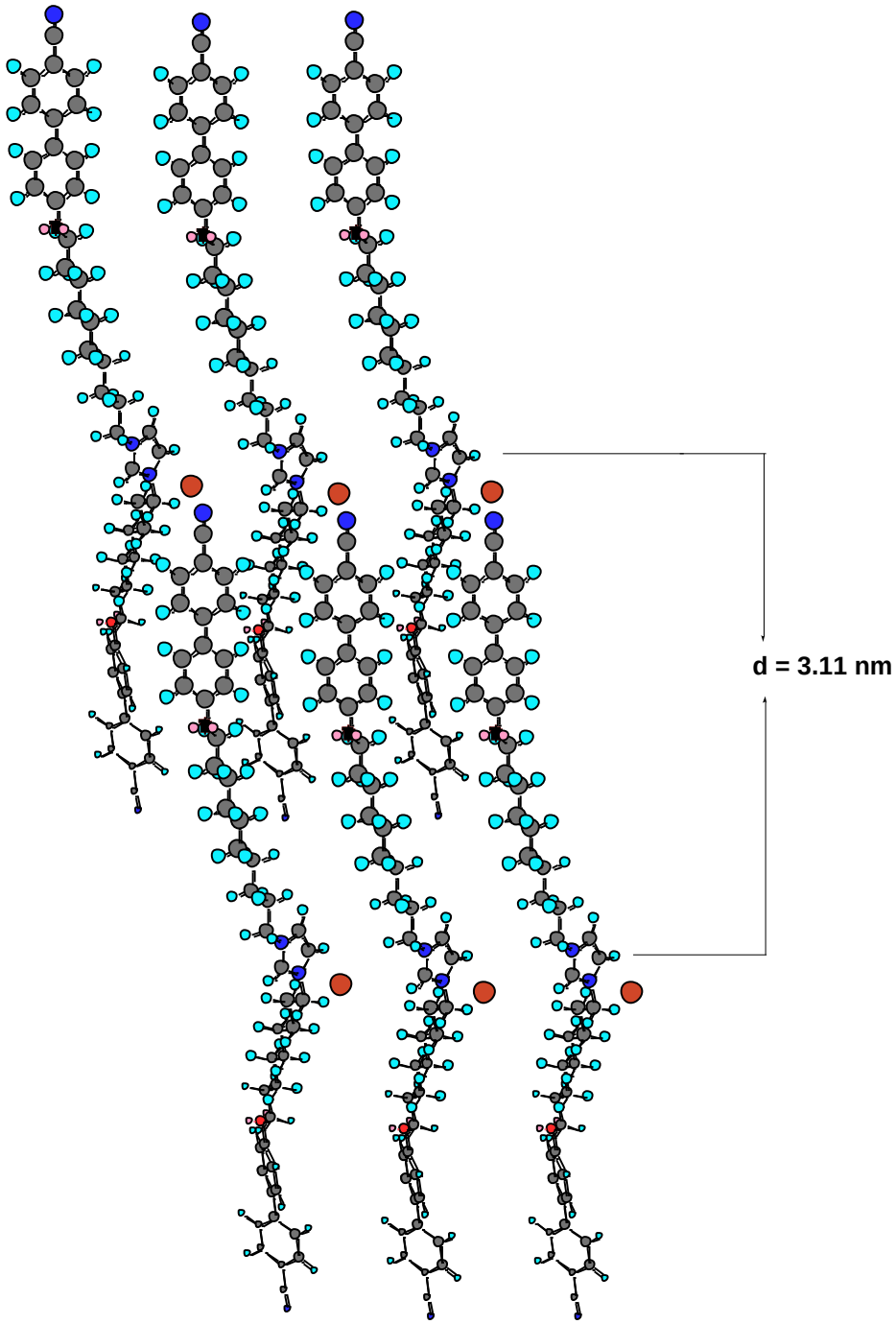

Figure 25. Sketch of intercalated SmA exhibited by **28d**.

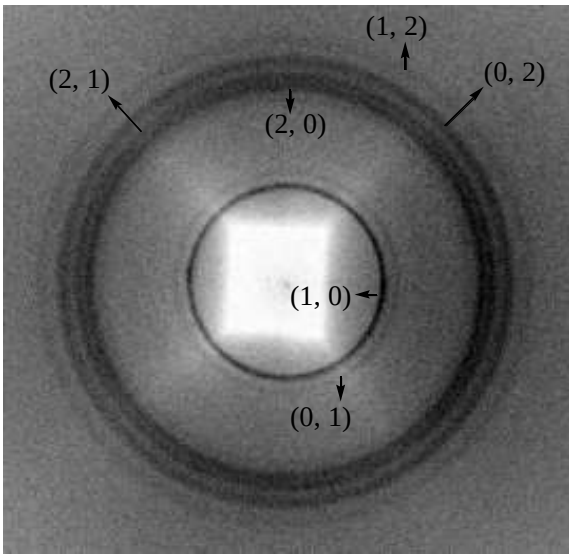

Figure 26. X-ray diffraction pattern obtained for compound **32** at room temperature.

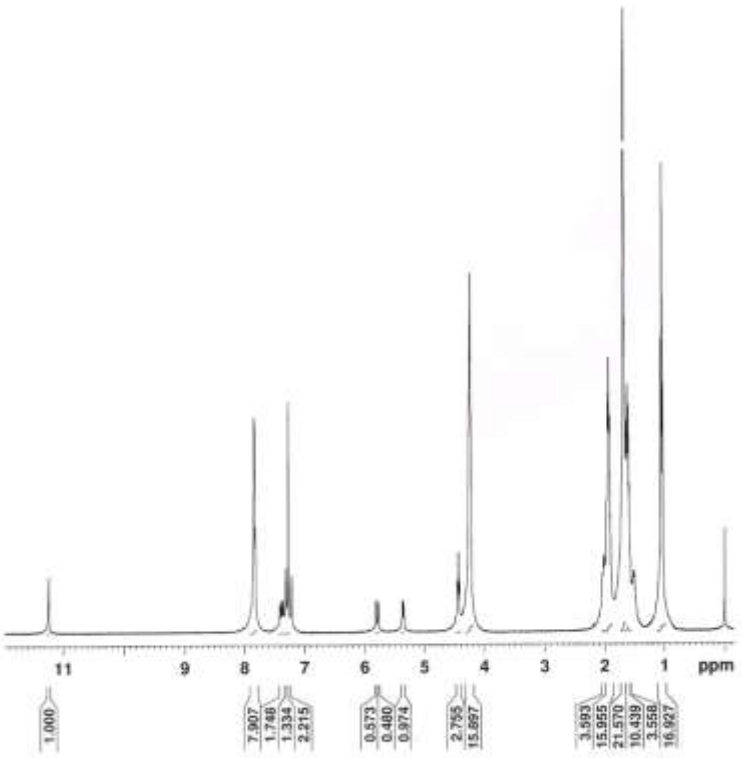

Figure 27. ^{1}H NMR spectrum of the compound **37**.

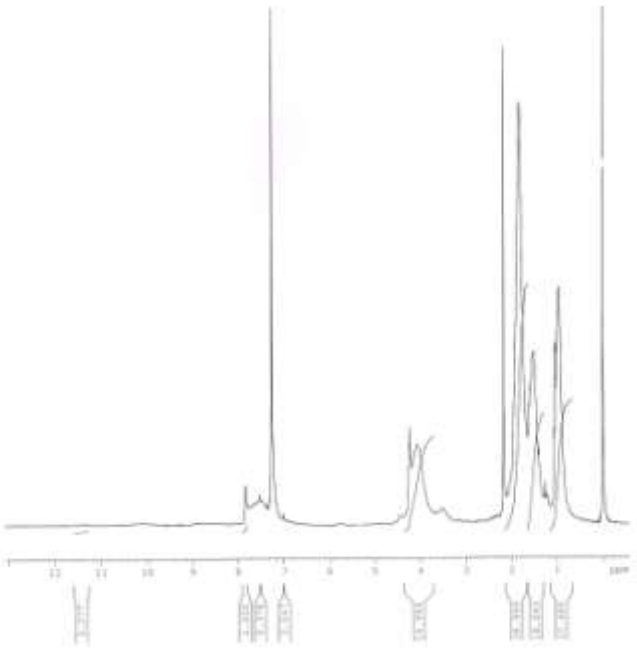

Figure 28. ^{1}H NMR spectrum of the polymer **38**.

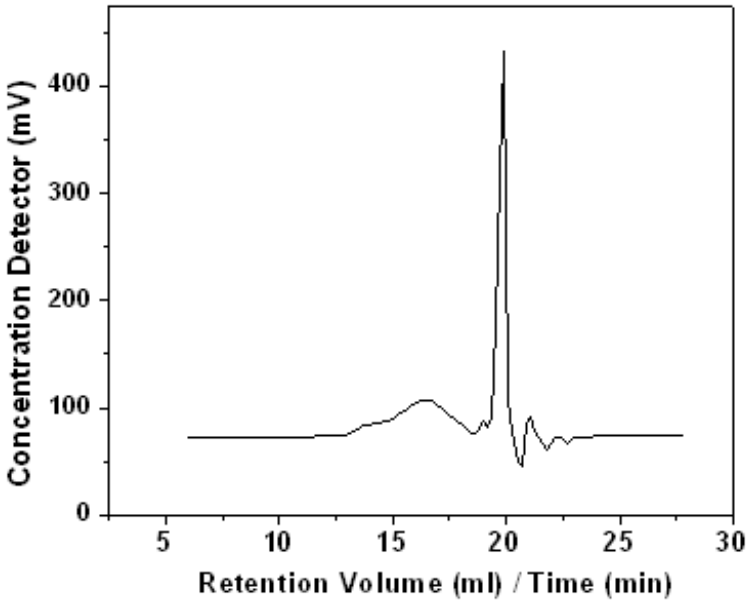

Figure 29. GPC of the ionic polymer **38** with respect to polystyrene standard.

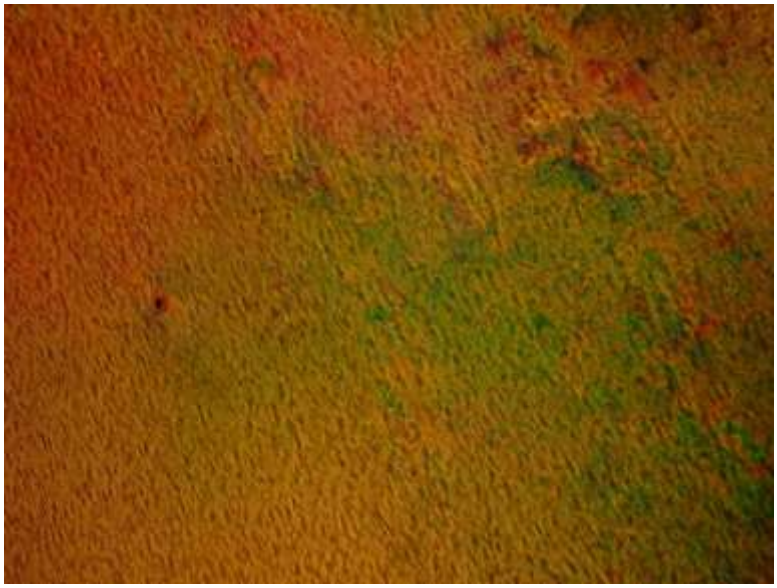

Figure 30. Optical photomicrograph of compound **38** at 195 ºC on cooling from isotropic liquid (Crossed polarizers, magnification X 200).

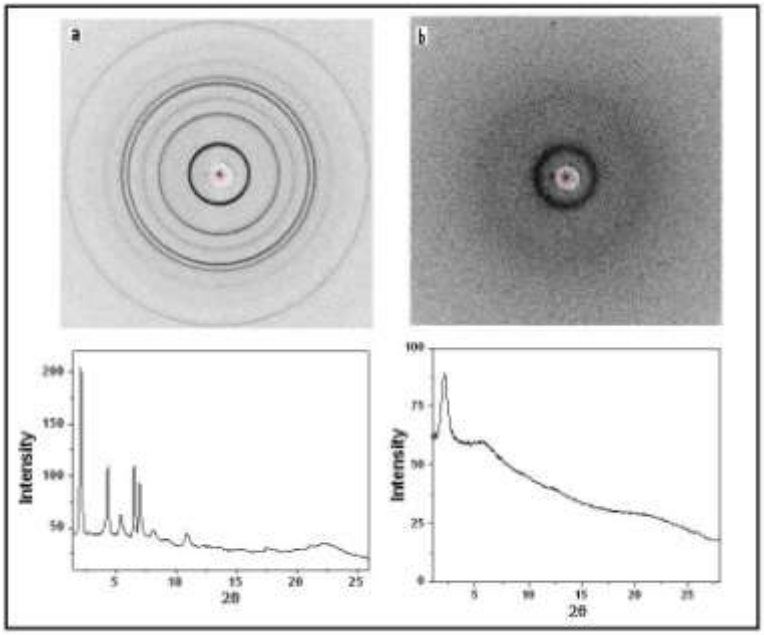

Figure 31. X-ray diffraction patterns and their intensity vs. 2θ plots obtained for (a) monomer (**37**) and (b) polymer (**38**) at 60 ºC and room temperature, respectively.